

AD-A073 340

AEROSPACE CORP EL SEGUNDO CA AEROTHERMODYNAMICS DEPT

F/6 16/3

A NUMERICAL SOLUTION FOR TEMPERATURE DISTRIBUTIONS IN A DISCRET--ETC(U)

AUG 79 A R KARAGOZIAN

F04701-78-C-0079

UNCLASSIFIED

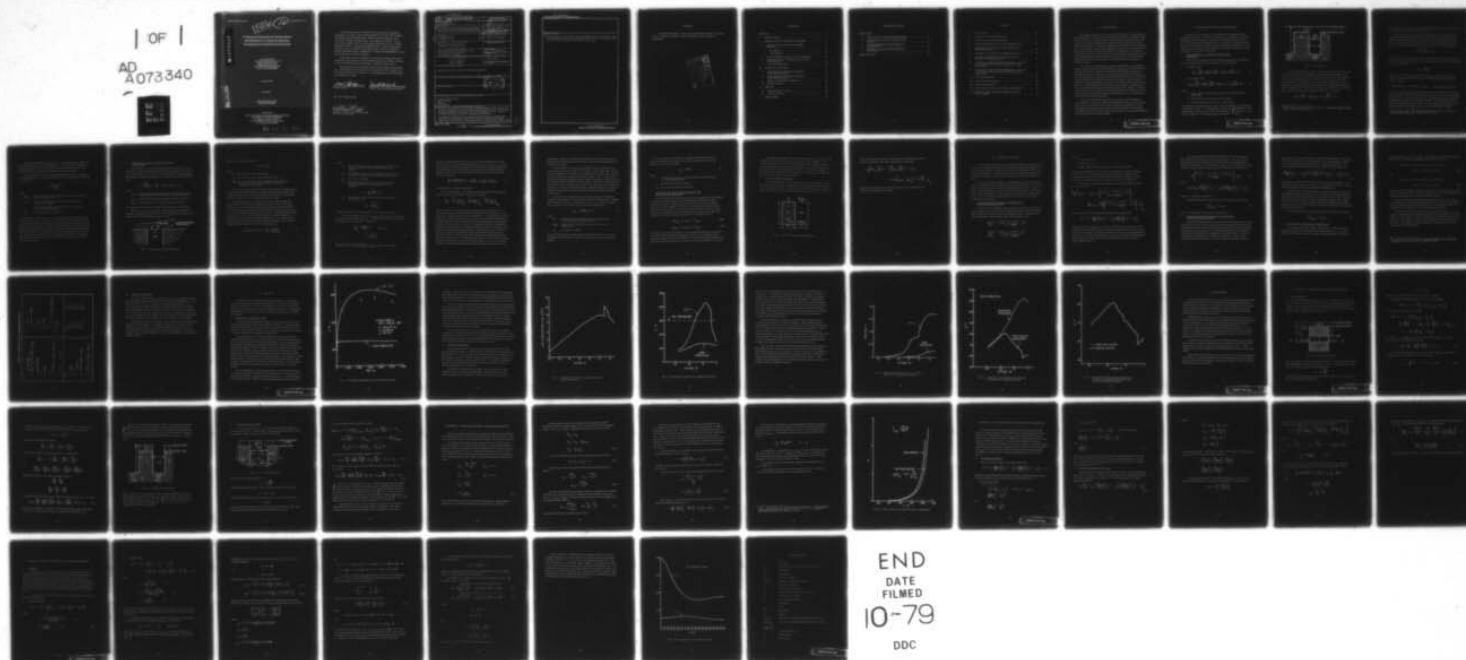
TR-0079(4550-73)-1

SAMSO-TR-79-52

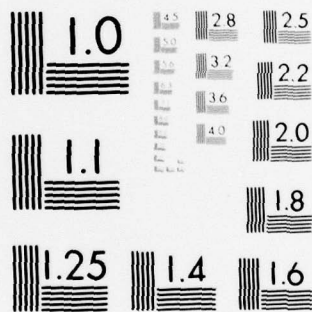
NL

| OF |

AD
A073340



END
DATE
FILMED
10-79
DDC



MICROCOPY RESOLUTION TEST CHART
 NATIONAL BUREAU OF STANDARDS-1963-A

LEVEL II

12

AD A 073340

A Numerical Solution for Temperature Distributions in a Discrete Injection Transpiration-Cooled Nostip System

A. R. KARAGOZIAN
Aerothermodynamics Department
Vehicle Engineering Division
Engineering Science Group
THE AEROSPACE CORPORATION
El Segundo, California 90245

DDC
AUG 30 1979
RECEIVED

20 August 1979

Final Report

APPROVED FOR PUBLIC RELEASE;
DISTRIBUTION UNLIMITED

DDC FILE COPY

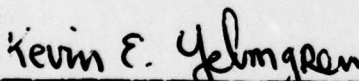
Prepared for
SPACE AND MISSILE SYSTEMS ORGANIZATION
AIR FORCE SYSTEMS COMMAND
Los Angeles Air Force Station
P.O. Box 92960, Worldway Postal Center
Los Angeles, Calif. 90009

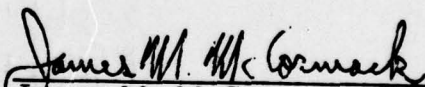
79 08 30 005

This final report was submitted by The Aerospace Corporation, El Segundo, CA 90245, under Contract F04701-78-C-0079 with the Space and Missile Systems Organization, Deputy for Reentry System, P.O. Box 92960, Worldway Postal Center, Los Angeles, CA 90009. It was reviewed and approved for The Aerospace Corporation by E. G. Hertler, Principal Director, AeroEngineering Subdivision, Vehicle Engineering Division, and R. E. Herold, Principal Director, Reentry Technology, Reentry Systems Division. Captain K. E. Yelmgren, SAMSO/RSEE, was the project engineer for Reentry Systems.


This report has been reviewed by the Information Office (OI) and is releasable to the National Technical Information Service (NTIS). At NTIS, it will be available to the general public, including foreign nations.

This technical report has been reviewed and is approved for publication. Publication of this report does not constitute Air Force approval of the report's findings or conclusions. It is published only for the exchange and stimulation of ideas.


Kevin E. Yelmgren, Capt, USAF
Project Officer


James M. McCormack, Lt Col, USAF
Chief, Reentry Technology Division

FOR THE COMMANDER


William Goldberg, Col., USAF
Director, Reentry Systems Technology
Deputy for Technology

UNCLASSIFIED

SECURITY CLASSIFICATION OF THIS PAGE (When Data Entered)

REPORT DOCUMENTATION PAGE		READ INSTRUCTIONS BEFORE COMPLETING FORM	
1. REPORT NUMBER SAMSO-TR-79-52	2. GOVT ACCESSION NO.	3. RECIPIENT'S CATALOG NUMBER 9	
4. TITLE (and Subtitle) A NUMERICAL SOLUTION FOR TEMPERATURE DISTRIBUTIONS IN A DISCRETE INJECTION TRANSPIRATION-COOLED NOSETIP SYSTEM		5. TYPE OF REPORT & PERIOD COVERED Final Rept. June 1978-Sept. 1978	
7. AUTHOR(s) A. R. Karagozian		6. PERFORMING ORG. REPORT NUMBER TR-0079(4550-73)-1	8. CONTRACT OR GRANT NUMBER(s) F04701-78-C-0079
9. PERFORMING ORGANIZATION NAME AND ADDRESS The Aerospace Corporation El Segundo, California 90245		10. PROGRAM ELEMENT, PROJECT, TASK AREA & WORK UNIT NUMBERS	
11. CONTROLLING OFFICE NAME AND ADDRESS Space and Missile Systems Organization Air Force Systems Command Los Angeles, CA 90009		12. REPORT DATE 20 August 1979	
14. MONITORING AGENCY NAME & ADDRESS (if different from Controlling Office) 1262p.		13. NUMBER OF PAGES 60	
		15. SECURITY CLASS. (of this report) Unclassified	
		15a. DECLASSIFICATION/DOWNGRADING SCHEDULE	
16. DISTRIBUTION STATEMENT (of this Report) Approved for public release; distribution unlimited.			
17. DISTRIBUTION STATEMENT (of the abstract entered in Block 20, if different from Report) DDIC RECEIVED AUG 31 1979 RECEIVED C			
18. SUPPLEMENTARY NOTES			
19. KEY WORDS (Continue on reverse side if necessary and identify by block number) Transpiration Cooling Mass Transfer Blowing Slot Cooling			
20. ABSTRACT (Continue on reverse side if necessary and identify by block number) An analysis is performed to describe the thermodynamics behavior of "fin" and fluid components of a transpiration-cooled nosetip system. Partial differential equations governing fin and fluid temperatures are derived and solved numerically to yield time-dependent distributions. Correlations used for the subcooled boiling heat transfer mechanism are found to over-predict the amount of heat removed from the fin in depth. A comparison of temperature distributions indicates that the fluid equation may			

DD FORM 1473
(IF ACQUISITION)

410528

UNCLASSIFIED
SECURITY CLASSIFICATION OF THIS PAGE (When Data Entered)

UNCLASSIFIED

SECURITY CLASSIFICATION OF THIS PAGE(When Data Entered)

19. KEY WORDS (Continued)

20. ABSTRACT (Continued)

be considered as steady state with a negligible effect on the solution. The numerical scheme used to solve the governing equations is strongly stable, even when drastic changes in parameters occur.

UNCLASSIFIED

SECURITY CLASSIFICATION OF THIS PAGE(When Data Entered)

PREFACE

The author would like to express her appreciation to Peter G. Crowell for his valuable contributions to the preparation of this document for publication.

Accession For	
WFO G&I	<input checked="checked" type="checkbox"/>
DDO TAB	<input type="checkbox"/>
Unannounced	<input type="checkbox"/>
Justification	<input type="checkbox"/>
By _____	
Distribution/	
Availability Codes	
Dist	Avail and/or special
A	

CONTENTS

PREFACE	1
I. INTRODUCTION	7
II. FORMULATION OF THE PHYSICAL MODEL	9
A. One-Dimensional Transient Conduction Equations	9
1. Fin Equation	9
2. Fluid Equation.	9
B. Surface Boundary Condition for the Fin Equation	13
C. Backface Boundary Conditions for the Fin and Fluid Equations	18
D. Global Energy Balance	19
III. NUMERICAL ANALYSIS	21
A. Fin Equation and Boundary Conditions in Finite Difference Form	21
B. Fluid Equation and Boundary Condition in Finite Difference Form	23
C. Solution of the System of Equations	24
D. Stability Analysis	27
IV. RESULTS	29
A. Ballistic Range Test Case	29
B. Flight Trajectory.	31
V. CONCLUSIONS.	39

CONTENTS (Continued)

APPENDICES:

A.	DERIVATION OF GOVERNING EQUATIONS	41
B.	VAPORIZATION FROM A LIQUID WATER SURFACE	47
C.	QUASILINEARIZED FORMULATION OF PARAMETERS	53
D.	STABILITY ANALYSIS FOR SYSTEM OF EQUATIONS	59
	NOMENCLATURE	67

FIGURES

1.	Fin Geometry	10
2.	Surface Mass Transfer Schematic	13
3.	Control Volume for Energy Balance	19
4.	Fin Surface Temperature for AEDC Ballistic Range	30
5.	Stagnation Points for Ideal Coolant Requirements (Kwajalein Mission)	32
6.	Fin Surface Temperature for Flight Environment	33
7.	Influence of Boiling Heat Transfer Model on Fin Erosion for Flight Environment	35
8.	Comparison of Fluid Surface Temperatures, Transient versus Steady-State Numerical Solution for Flight Environment	36
9.	Comparison of Fluid Surface Temperatures, Transient versus Steady-State Numerical Solution for Flight Environment	37
A-1.	Fin Volume Element	41
A-2.	Control Volume Geometry	44
A-3.	Fluid Volume Element	45
B-1.	Mass Transfer Parameter for Water Vaporization	51
D-1.	Stability Analysis for System Eigenvalues versus Phase Angle β	65

I. INTRODUCTION

The purpose of this report is to present the results of an examination of the thermodynamic performance of the discrete injection transpiration-cooled nosetip (TCNT) for reentry vehicles. By analyzing the physical model of the system numerically, predictions for nosetip surface temperatures during flight may be obtained. Test data indicate that in the case of a reentry vehicle clear air trajectory, aerodynamic heating alone can cause the temperature of the nosetip to increase beyond the material's melting point. In an environment where particles of snow or dust impinge upon the nosetip surface, it has been found that erosion of the surface is more prevalent. The model which describes the system must therefore take into account the possibility of a receding surface.

An underlying assumption in the physical description of the problem is that the plate-like elements which compose the nosetip may be represented as individual webs (fins), while the coolant flowing through the nosetip flow passageways may be considered to absorb energy from the individual fins, with the coolant then removing heat by flowing out of the system. The energy balance described in Appendix A results in two coupled, one-dimensional transient heat conduction equations which involve temperatures of the fin and the fluid. Surface heat fluxes, which become part of the fin boundary conditions, are taken to be those at the stagnation point of the nosetip. The fin is represented as a semi-infinite slab, thus implying that the distance from the nosetip surface to the orifice through which coolant enters is much greater than the thermal penetration depth.

An implicit finite difference scheme is used to solve the equations numerically on a computer. Iterative techniques are incorporated to ensure that dramatic parameter changes (either in boundary conditions or in the coupling of the equations) do not drive the system unstable. Temperature distributions for clear air and weather environments are compared with actual test data recorded in a ballistic range.

II. FORMULATION OF THE PHYSICAL MODEL

The nature of this problem is such that fin and fluid temperatures influence one another. If the fin temperature T_F is a function of time due to changing surface conditions, it may be concluded that the "bulk" temperature of the fluid T_B also changes with time. Separate energy balances are performed in Appendix A to yield two partial differential equations. For the purposes of this analysis, the fin material is assumed to be stainless steel, and the fluid is considered to be water.

A. ONE-DIMENSIONAL TRANSIENT CONDUCTION EQUATIONS

The governing equations for fin and fluid temperatures as functions of time and distance are derived in Appendix A and shown below.

1. FIN EQUATION:

$$\rho_F C_{PF} \frac{\partial T_F}{\partial t} = \frac{\partial}{\partial x} \left(K_F \frac{\partial T_F}{\partial x} \right) + (\rho_F C_{PF} \dot{s}) \frac{\partial T_F}{\partial x} + \frac{2}{a} \cdot Q \quad (1)$$

2. FLUID EQUATION:

$$\rho_B C_{PB} \frac{\partial T_B}{\partial t} = \frac{\partial}{\partial x} \left(K_B \frac{\partial T_B}{\partial x} \right) + (\rho_B C_{PB} \dot{s} + \dot{m} C_{PB}) \frac{\partial T_B}{\partial x} - \frac{2}{b} \cdot Q \quad (2)$$

where

$Q = h(T_B - T_F)$, the internal convective heat transfer rate per unit length

\dot{s} = the recession or erosion rate of fin surface

\dot{m} = the mass flow rate per unit area of the coolant

The dimensions and other terms refer to the representation of the physical model shown in Fig. 1. The dimensions a' and b' are substituted for a and b , respectively, in the equations when x lies between $l - \int_0^t \dot{s} dt$ and l . Also, for this range of x , \dot{m}' should replace \dot{m} , where $\dot{m}' = \dot{m} b/b'$.

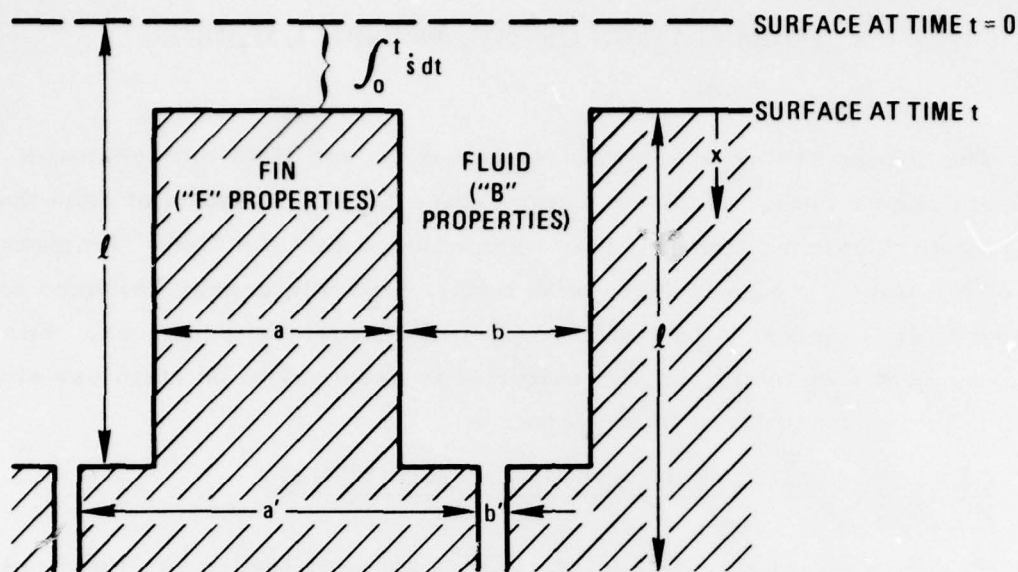


Fig. 1. Fin Geometry

It is apparent that in the fluid, energy is transported in the flow direction by both convection and conduction. The Peclet number ($D\rho UC_P/K$) provides a measure of the relative importance of convection to conduction and, for the conditions of interest, has a minimum value on the order of several hundred. Calculations done to assess the importance of axial conduction have indicated¹ that the error involved in dropping the conduction term is negligible for values of the Peclet number greater than one hundred. Thus, with the deletion of the conduction term, Eq. (2) becomes

$$\rho_B C_{PB} \frac{\partial T_B}{\partial t} = (\rho_B C_{PB} \dot{s} + \dot{m} C_{PB}) \frac{\partial T_B}{\partial x} - \frac{2}{b} \cdot Q \quad (3)$$

¹ Ralph P. Stein, "Liquid Metal Heat Transfer," Advances in Heat Transfer, Vol. 3, Academic Press (1966).

This revised fluid equation simplifies the numerical analysis and aids in the spatial stabilization of the fluid temperatures.

The source term Q is dependent upon the type of heat transfer mechanism that couples the fin to the coolant. In this case, either heat transfer without phase change of the fluid or subcooled boiling heat transfer is postulated. When no phase change occurs, that is, when the temperature of the fin is less than the saturation temperature of the fluid, Q takes the form

$$Q = \frac{Nu \cdot K_B}{D_H} (T_B - T_F)$$

where Nu is the Nusselt number, and has been assigned an average value of 4 for the ballistic range and flight cases reported herein; and D_H is the hydraulic diameter, determined as

$$D_H = \frac{2b}{1 + b/w}$$

where w is the width of the fluid and fin elements. As an estimate for the subcooled boiling heat transfer rate, an empirical relation postulated by Thom² is used:

$$Q(\text{Btu/ft}^2\text{-sec}) = 0.0536 e^{\tilde{P}} (T_F - T_{SAT})^2 \quad (\text{temperatures are in } ^\circ\text{R})$$

where T_{SAT} is the saturation temperature of the coolant (found as a function of the external pressure and \tilde{P} is defined to be $P/630$, where P is the external pressure in psia. For the case where T_F is greater than T_{SAT} , Q should be calculated using both of the foregoing relations. The larger value is then chosen to represent the source term, since the heat transfer mechanism for subcooled boiling is greatly improved over that without phase change.

² J.R.S. Thom, et al., "Boiling in Subcooled Water in Tubes and Anulli," Proc. Institute Mech. Eng., 3C180:226 (1965-1966).

It has been suspected from prior usage that the equation for subcooled boiling heat transfer is overly optimistic, i.e., the equation overpredicts the amount of heat removed from the fin. For the present, however, this relation shall be used until new correlations can be formulated.

The erosion rate of the fin \dot{s} depends upon the free-stream conditions outside the shock wave. An empirical formula used to obtain the erosion rate is as follows:

$$\dot{s} = \frac{\frac{1}{2} \rho_{LWC} U_{\infty}^3}{C_N \rho_F}$$

where

ρ_{LWC} = the liquid water content of the free stream (the mass of water per volume of air)

U_{∞} = the free-stream velocity, which is equivalent to the velocity of the vehicle

C_N = an erosion coefficient, herein taken to be a function of the fin surface temperature

ρ_F = the density of the fin material

For the purposes of this analysis, it is assumed that in a clear air environment the erosion term is always zero. At present, the formulation does not model fin material thermally removed when surface temperatures exceed the material melt temperature. The important information to be obtained in the clear air case is whether or not the fin surface temperature actually reaches the melt temperature. The value for mass flux of the coolant \dot{m} is assumed to be supplied as a function of time or altitude of the vehicle. Coolant mass flux will be specified by design to restrict surface temperature to below material melt values.

B. SURFACE BOUNDARY CONDITION FOR THE FIN EQUATION

The second-order partial differential equation which governs the temperature in the fin indicates that two boundary conditions are needed for complete solution. The surface condition in the fin is dependent upon the net heat flux conducted into the fin. The boundary condition takes the form:

$$-K_F \left. \frac{\partial T_F}{\partial x} \right|_{x=0} = \dot{q}_{\text{net}} = \dot{q}_{\text{aero}} + \dot{q}_{\text{part}} - \dot{q}_{\text{rad}} \quad (4)$$

where

\dot{q}_{aero} = the aerodynamic heat flux at the fin surface, taking into account injection of the fluid into an air boundary layer

\dot{q}_{part} = the heat flux due to the impinging of weather particles

\dot{q}_{rad} = the heat flux due to radiation from the fin surface

These heat flux terms may be evaluated by the analysis which follows.

Because some percentage of the coolant vaporizes at the fluid-air interface, a boundary layer composed of air, H_2O liquid, and H_2O vapor is formed over the TCNT surface as shown in Fig. 2.

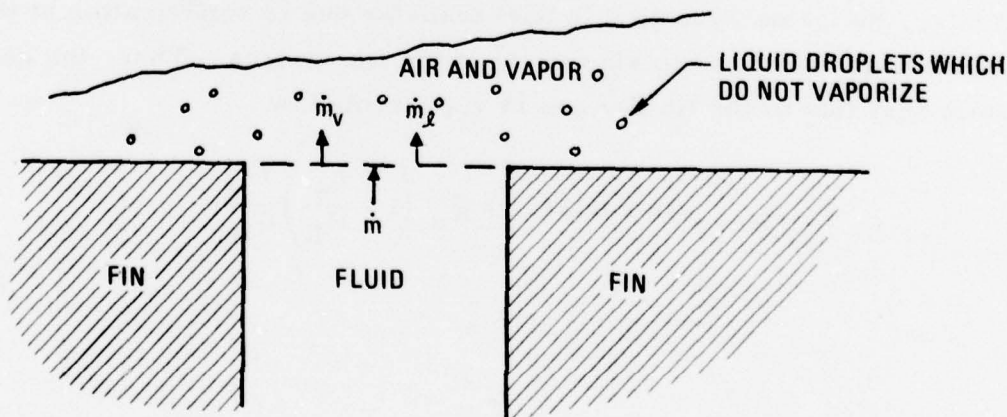


Fig. 2. Surface Mass Transfer Schematic

Here the relationship holds that

$$\dot{m} = \dot{m}_v + \dot{m}_l$$

where

\dot{m} = the total mass flux of the coolant

\dot{m}_v = the mass flux of the coolant which vaporizes

\dot{m}_l = the mass flux of the coolant which does not vaporize at the liquid-air interface and therefore enters the boundary layer as a liquid

The surface temperatures of both the fluid and fin are sufficiently low and the pressure sufficiently high to preclude the possibility of gas phase reactions at the surface. Thus, the only gas phase species present at the surface are water vapor, molecular nitrogen, and oxygen.

The width of the fin is assumed to be small enough such that the boundary layer does not relax significantly from its state over the slot. That is, it is assumed that the aerodynamic heat flux to the fin surface is essentially the same as the heat flux to the fluid issuing from the upstream slot. The only difference between the two values is that the heat flux to the fin surface is corrected to reflect the higher fin surface temperature. In particular, the same reduction in heat transfer due to vaporization at the slot surface is presumed to also apply at the fin surface. Thus, the aerodynamic heat flux to the fin surface is represented by

$$\dot{q}_{\text{aero}}(\text{fin surface}) = \dot{q}_o \left(1 - \frac{h_w}{H_R} \right) \frac{C_H}{C_{H_o}} \quad (5)$$

where

\dot{q}_o = the cold-wall, non-blown aerodynamic heat flux to the surface (evaluated at the stagnation point in this report)

h_w = the enthalpy of the mixture of species at the wall surface (therefore evaluated at the fin surface temperature)

H_R = the recovery enthalpy

C_H = the Stanton number for heat transfer with blowing (assumed equal to the Stanton number for mass transfer)

$$C_H = \frac{\dot{q}_{aero}}{\rho_e u_e (H_R - h_w)}$$

C_{H_o} = the Stanton number in the limit for non-blown heat transfer ($\dot{m}_v = 0$)

$$C_{H_o} = \frac{\dot{q}_o}{\rho_e u_e H_R}$$

The terms in Eq. (5) may be determined in the following manner.

The ratio of Stanton numbers, C_H/C_{H_o} , is by definition a function of the mass transfer driving force, B' . A commonly used expression, with some theoretical justification³, is given by

$$\frac{C_H}{C_{H_o}} = \frac{\ln(\lambda B' + 1)}{\lambda B'} \quad (\lambda = 1.28)$$

$$B' \equiv \frac{\dot{m}_v}{\rho_e u_e C_H} \quad (6)$$

³W. H. Dorrance, Viscous Hypersonic Flow, McGraw-Hill (1962).

The ratio of Stanton numbers is also known to be the "blowing correction" for the mass flux of the coolant which vaporizes at the surface, \dot{m}_v . Following the analysis described in Appendix B, the Knudsen-Langmuir equation for non-equilibrium water vaporization is incorporated to yield the following equation, which may be solved iteratively for B' for given values of fluid surface temperature

$$\left(\beta + \frac{B'}{18}\right) \frac{\ln(\lambda B' + 1)}{\lambda} + G \frac{B'}{18} (P - P_{H_2O}^v) = G \beta P_{H_2O}^v \quad (7)$$

The variables are defined in Appendix B.

The "wall enthalpy" h_w is a function of the enthalpies of the individual species present at the surface, so that we may write

$$\frac{h_w}{RT_F} = \frac{K_{O_2}}{32} \left(\frac{H}{RT_F}\right)_{O_2} + \frac{K_{N_2}}{28} \left(\frac{H}{RT_F}\right)_{N_2} + \frac{K_{H_2O}}{18} \left(\frac{H}{RT_F}\right)_{H_2O}$$

where the species mass fractions (K_i) existing at the fin surface are presumed to be the same as those at the slot surface and are evaluated in terms of the mass transfer parameter B' (see Appendix B). The temperature used to evaluate h_w is that of the fin surface, since it is assumed that the gas phase adjacent to the wall adjusts instantaneously to the step change in temperature from the fluid value to the fin value. It is recognized that this instantaneous relaxation in temperature is inconsistent with the previous assumption of slow relaxation with respect to surface blowing. This inconsistency is tolerated because it provides a mechanism for the fin aerodynamic heat flux to be influenced by the fin surface temperature (which seems physically plausible, at least to some degree). A better approach would be to use weighted averages of surface temperature and mass transfer parameter, in terms of relaxation distances, to determine the wall temperature and blowing corrections to the

fin heat flux. However, in light of the boiling heat transfer and two-phase boundary layer uncertainties in the analysis, this additional complexity does not seem warranted.

The parameters H_R and \dot{q}_o may be obtained from an analysis of the boundary layer flowing over the TCNT nosetip. In this report, the values of recovery enthalpy and cold wall, non-blowing heat flux will be taken as those values appropriate to a gaseous air boundary layer. That is, the coolant mass flux entering the boundary layer as liquid water \dot{m}_l is assumed to exert no influence upon the heat flux to the fin surface. This is obviously incorrect, but it does provide an upper bound for the surface heat flux and is justified on that basis. An analysis of the two-phase air-water boundary layer would be required to accurately define the heat flux and is beyond the scope of the present effort.

The flux at the fin surface due to particle heating \dot{q}_p will enter the boundary condition [Eq. (4)] when ambient conditions indicate that a "weather environment" is present. For particles of rain or snow, the particle heat flux is a function of the liquid water content of the atmosphere

$$\dot{q}_{\text{part}} = \frac{1}{2} \alpha \rho_{\text{LWC}} (U_{\infty})^3 \quad (8)$$

where

α = accommodation coefficient, which is experimentally determined (herein assumed to be 0.7)

ρ_{LWC} = liquid water content with units of mass of water per volume of air

U_{∞} = free-stream velocity

Since the weather test case that shall be considered later does not include impingement of dust particles, Eq. (8) will be used to represent particle heating.

The radiative term in boundary condition [Eq. (4)] usually will be much smaller than the aerodynamic or particle heat fluxes, but for completeness is evaluated as follows:

$$\dot{q}_{\text{rad}} = \epsilon \sigma T_F^4 \quad (9)$$

where

ϵ = the total hemispherical emissivity of the fin assumed to be 0.16 (for stainless steel)

σ = the Stefan-Boltzmann constant

T_F = the surface temperature of the fin

C. BACKFACE BOUNDARY CONDITIONS FOR THE FIN AND FLUID EQUATIONS

The second boundary condition used for the fin equation and the boundary condition for the fluid equation are both specified at the backface of the respective elements. Both elements are considered to be semi-infinite slabs; that is, the length l is assumed to be much greater than the thermal penetration depth of either fin or fluid for the time scale of interest. Thus, the backface temperatures remain at their initial values for the entire time considered, so that our boundary conditions are formulated to be

$$T_F \Big|_{x=l} = T_{F \text{ initial}} = T_{\text{initial}} \quad (10a)$$

$$T_B \Big|_{x=l} = T_{B \text{ initial}} = T_{\text{initial}} \quad (10b)$$

So that no convective heat transfer occurs at the lower portion of our model, we assume that the initial temperatures of the fin and the fluid are equal. Since the reentry vehicle is in storage for a considerable length of time before being used, the fin and fluid are assumed to be at room temperature initially.

An alternate formulation of these boundary conditions is to consider the conduction in both the fin and the fluid to be zero at the backface. This condition is perfectly valid for the semi-infinite slab assumption; however, since conduction in the fluid is neglected anyway, it provides redundancy as a backface fluid boundary condition. Since we wish to have the backface temperatures for both elements in equilibrium, the relations Eq. (10a) and Eq. (10b) will be applied to the problem.

D. GLOBAL ENERGY BALANCE

In order to check the validity of the temperature distributions obtained by solution of the two governing equations, an overall energy balance of the system should be satisfied. We consider a control volume for the entire system (composed of one fin element and one fluid element) as shown in Fig. 3.

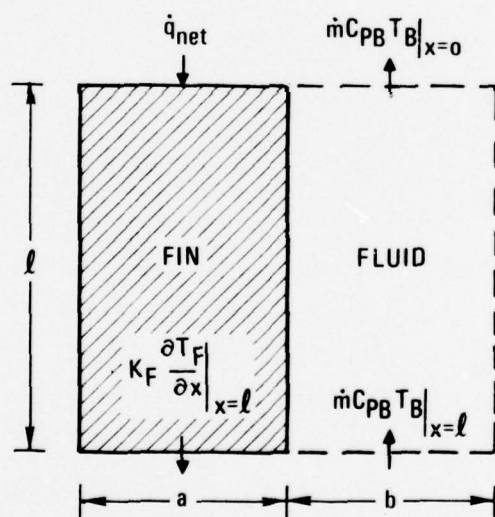


Fig. 3. Control Volume for Energy Balance

The net energy into the system must be equal to the change in sensible energy in the fin and in the fluid, yielding the relationship

$$\begin{aligned}
 a \int_0^l \rho_F C_{PF} \frac{\partial T_F}{\partial t} dx + b \int_0^l \rho_B C_{PB} \frac{\partial T_B}{\partial t} dx = a \dot{q}_{\text{net}} + \\
 + b \dot{m} C_{PB} \left(T_B \Big|_{x=l} - T_B \Big|_{x=0} \right) - a K_F \frac{\partial T_F}{\partial x} \Big|_{x=l}
 \end{aligned}
 \tag{11}$$

Equation (11) shall be used to test the accuracy of the finite difference solution of the differential equations.

III. NUMERICAL ANALYSIS

The two coupled partial differential equations which govern the behavior of the fin and fluid temperatures must be solved by numerical methods. An implicit finite difference scheme shall be used to represent the terms in the differential equations. An explicit formulation was initially attempted, but numerical instabilities caused a quick reversion to the method finally employed.

The basic principle underlying an implicit finite difference representation of a partial differential equation is that the spatial derivatives are represented as functions of the dependent variable at the future time. Thus, to obtain spatially dependent values of the variable from one time level to the next, a system of equations must be solved. As the time and spatial increments used in the difference approximation become smaller, the values approach the true solution.

A. FIN EQUATION AND BOUNDARY CONDITIONS IN FINITE DIFFERENCE FORM

In order to ensure stability of the solution even with severe heat fluxes at the fin surface, a variable spatial increment will be incorporated to produce a tighter mesh at the surfaces of both fin and fluid. The three-point central difference representations with variable mesh size are

$$\left. \frac{\partial T}{\partial x} \right|_j^{n+1} = \frac{R^2 T_{j+1}^{n+1} + (1 - R^2) T_j^{n+1} - T_{j-1}^{n+1}}{(1 + R) R \Delta x_j}$$

$$\left. \frac{\partial^2 T}{\partial x^2} \right|_j^{n+1} = \frac{R T_{j+1}^{n+1} - (1 + R) T_j^{n+1} + T_{j-1}^{n+1}}{\frac{1}{2} (1 + R) R (\Delta x_j)^2}$$

where

j = the spatial node

n = the time level

$R \equiv \Delta x_{j-1} / \Delta x_j$, the ratio of successive spatial increments

An iterative technique shall be employed to determine parameters at future time levels. Thus, quasi-linearization may be used to represent more accurately those parameters which change dramatically with time. Quasi-linearized formulations of these parameters are derived in Appendix C.

The resulting implicit finite difference representation of the fin equation is as follows:

$$\begin{aligned} \frac{\rho_{FCPF}^i}{\Delta t} \left\{ T_{F_j}^{i+1} - T_{F_j}^n \right\} = K_F^i \left\{ \frac{RT_{F_{j+1}}^{i+1} - (1+R)T_{F_j}^{i+1} + T_{F_{j-1}}^{i+1}}{\frac{1}{2}(1+R)R(\Delta x_j)^2} \right\} \\ + \left(\rho_{FCPF}^i + \frac{\partial K_F^i}{\partial x} \right) \left\{ \frac{R^2 T_{F_{j+1}}^{i+1} + (1-R^2)T_{F_j}^{i+1} - T_{F_{j-1}}^{i+1}}{(1+R)R\Delta x_j} \right\} + \frac{2}{a} Q_j^{i+1} \end{aligned} \quad (12)$$

where i denotes the level of iteration of the set of equations and

$$Q_j^{i+1} \equiv Q_j^i + \left(\frac{\partial Q}{\partial T_F} \right)_j^i \left(T_{F_j}^{i+1} - T_{F_j}^i \right) + \left(\frac{\partial Q}{\partial T_B} \right)_j^i \left(T_{B_j}^{i+1} - T_{B_j}^i \right)$$

which is derived in Appendix C. Iteration of the system of equations is performed until the difference between successive temperature iterations is less than some established convergence criterion. Since some of the properties in Eq. (12) do not change dramatically as a function of temperature (specifically, the properties of steel), they may be approximated as values at iteration level i rather than at $i+1$.

The surface boundary condition in the fin may also be represented in finite difference form because of the conduction term. Yet, if we assume that the first node ($j=1$) occurs at the surface of the fin, the temperature evaluation at the node $j-1$ has no meaning. Thus, a forward difference representation of the derivative shall be used for this boundary condition at $j=1$:

$$K_F^i \left\{ \frac{R^2 T_{F3}^{i+1} - (1+R)T_{F2}^{i+1} + (1+2R)T_{F1}^{i+1}}{(1+R)R\Delta x_2} \right\} = \dot{q}_{net}^{i+1} \quad (13)$$

where

$$\dot{q}_{net}^{i+1} = \dot{q}_{net}^i + \left(\frac{\partial \dot{q}_{net}}{\partial T_F} \right)_1^i (T_{F1}^{i+1} - T_{F1}^i) + \left(\frac{\partial \dot{q}_{net}}{\partial T_B} \right)_1^i (T_{B1}^{i+1} - T_{B1}^i)$$

which are evaluated in Appendix C.

The backface boundary condition in the fin is represented simply as

$$T_{F_{j=JMAX}}^{i+1} = T_{initial} \quad (14)$$

where $j = JMAX$ refers to the node at which $x = l$.

B. FLUID EQUATION AND BOUNDARY CONDITION IN FINITE DIFFERENCE FORM

Since the two equations governing fin and fluid temperatures are coupled by the source term Q , it follows that the time and spatial increments used to approximate the fluid equation should be the same as those in the fin equation. In addition, the sudden increase in Q (when the fin temperature exceeds the fluid saturation temperature) strengthens the coupling further, and incites oscillations in the temperature distributions with time. Hence, quasi-linearization of the source term is used to rectify this situation. Spatial

oscillations also tend to occur when a central difference scheme represents the spatial derivative in the fluid equation, thus necessitating the incorporation of a two-point forward difference (i.e., upwind differencing). The resulting implicit finite difference representation of the fluid equation is

$$\frac{\rho_B^i C_{PB}^i}{\Delta t} \left\{ T_{B_j}^{i+1} - T_{B_j}^n \right\} = \frac{(\dot{m} C_{PB}^i + \rho_B^i C_{PB}^i \dot{s})}{\Delta x_j} \left\{ T_{B_{j+1}}^{i+1} - T_{B_j}^{i+1} \right\} - \frac{2}{b} Q_j^{i+1} \quad (15)$$

where Q_j^{i+1} is expanded in the same manner as for the fin equation. The parameters ρ_B and C_{PB} are evaluated at increment level i by the assumption that fluid properties do not vary greatly with temperature.

While the use of the upwind difference scheme for the convective term eliminates the spatial oscillations, it is only first-order accurate spatially, whereas the central difference scheme is second-order accurate. However, sufficient accuracy may be ensured by using a fine mesh near the surface (i.e., $R < 1$). In any event, excessive concern with higher order accurate numerical schemes is hardly warranted when the uncertainties in the physical model drive the solution.

The backface boundary condition in the fluid is represented simply as

$$T_{B_{j=JMAX}}^{i+1} = T_{initial} \quad (16)$$

C. SOLUTION OF THE SYSTEM OF EQUATIONS

In examining the system of Eqs. (12) and (15), we find that the two dependent variables are evaluated at three spatial levels: $j-1$, j , and $j+1$. Thus, since the equations can be written in tridiagonal form, the unknown

future temperatures T_{Fj}^{i+1} and T_{Bj}^{i+1} may be found using established solution procedures.⁴ A system of tridiagonal equations takes the form

$$\begin{aligned} A(j, 1) u_{j+1} + A(j, 2) u_j + A(j, 3) u_{j-1} + A(j, 4) v_{j+1} + \\ + A(j, 5) v_j + A(j, 6) v_{j-1} = A(j, 7) \end{aligned} \quad (17a)$$

and

$$\begin{aligned} B(j, 1) u_{j+1} + B(j, 2) u_j + B(j, 3) u_{j-1} + B(j, 4) v_{j+1} + \\ + B(j, 5) v_j + B(j, 6) v_{j-1} = B(j, 7) \end{aligned} \quad (17b)$$

where u and v are dependent variables evaluated at time level $i+1$, the j values represent the nodal points, in this case varying from 1 to JMAX, and A and B represent coefficient arrays which are defined in Table 1.

Clearly, the two governing difference equations can be represented in this manner if the fin equation takes the form of Eq. (17a) with T_F replacing u and T_B replacing v and if the fluid equation takes the form Eq. (17b). The coefficients in the equations are listed on the following pages.

It is apparent that the surface boundary condition in the fin, Eq. (13), cannot be rearranged into tridiagonal form at $j=1$ since it contains a variable at the $j+2$ level. However, if solved simultaneously with the difference equation at $j=2$, the boundary condition can be manipulated to take the form of Eq. (17a). The backface boundary conditions in both equations are easily represented in tridiagonal form.

⁴R.D. Richtmyer and K.W. Morton, Difference Methods for Initial Value Problems, p. 276, Interscience Publishers (1967).

Table 1. Coefficient Arrays for Tridiagonal Equations

<p>$J = 2, JMAX-1:$</p> $A(j, 1) = \frac{K_F^i R}{D1} + \frac{\left(\rho_F^i C_{PF}^i + \frac{\partial K_F^i}{\partial x}\right) R^2}{D2}$ $A(j, 2) = \frac{-\rho_F^i C_{PF}^i}{\Delta t} - \frac{K_F^i (1+R)}{D1} + \frac{\left(\rho_F^i C_{PF}^i + \frac{\partial K_F^i}{\partial x}\right) (1-R^2)}{D2} + \frac{2}{a} \left(\frac{\partial Q}{\partial T_F}\right)^i_j$ $A(j, 3) = \frac{K_F^i R}{D1} - \frac{\left(\rho_F^i C_{PF}^i + \frac{\partial K_F^i}{\partial x}\right)}{D2}$ <p>$A(j, 4) = 0$</p> $A(j, 5) = \frac{2}{a} \left(\frac{\partial Q}{\partial T_B}\right)^i_j$ <p>$A(j, 6) = 0$</p> $A(j, 7) = \left[-\frac{\rho_F^i C_{PF}^i}{\Delta t} T_{F,j}^n + \frac{2}{a} \left[-Q_j^i + \left(\frac{\partial Q}{\partial T_F}\right)^i_j T_{F,j}^i + \left(\frac{\partial Q}{\partial T_B}\right)^i_j T_{B,j}^i \right] \right]$ <p>and</p> $D1 = \frac{1}{2} (1 + R) R (\Delta x_j)^2, \quad D2 = (1 + R) R \Delta x_j$	<p>$J = 1:$</p> $A(1, 1) = \frac{-R^2 A(2, 2)}{A(2, 1)} - (1 + R)^2$ $A(1, 2) = \frac{-R^2 A(2, 3)}{A(2, 1)} + (1 + 2R) - \left(\frac{\partial q_{net}}{\partial T_F}\right)^i_1 C$ <p>$A(1, 3) = 0$</p> $A(1, 4) = \frac{-R^2 A(2, 5)}{A(2, 1)}$ $A(1, 5) = -\left(\frac{\partial q_{net}}{\partial T_B}\right)^i_1 C$ <p>$A(1, 6) = 0$</p> $A(1, 7) = \frac{-R^2 A(2, 7)}{A(2, 1)} + C \left[q_{net}^i \left(\frac{\partial q_{net}}{\partial T_F}\right)^i_1 T_{F,1}^i + \left(\frac{\partial q_{net}}{\partial T_B}\right)^i_1 T_{B,1}^i \right]$ <p>where</p> $C = \frac{(1 + R) R \Delta x_2}{K_F^i}$
<p>$J = 1, JMAX-1:$</p> <p>$B(j, 1) = 0$</p> $B(j, 2) = \frac{-2}{b} \left(\frac{\partial Q}{\partial T_F}\right)^i_j$ <p>$B(j, 3) = 0$</p> $B(j, 4) = \frac{(\dot{m} C_{PB}^i + \rho_B^i C_{PB}^i s)}{\Delta x_j}$ $B(j, 5) = \frac{-\rho_B^i C_{PB}^i}{\Delta t} - \frac{(\dot{m} C_{PB}^i + \rho_B^i C_{PB}^i s)}{\Delta x_j} + \frac{2}{b} \left(\frac{\partial Q}{\partial T_B}\right)^i_j$ <p>$B(j, 6) = 0$</p> $B(j, 7) = \left[-\frac{\rho_B^i C_{PB}^i}{\Delta t} T_{B,j}^n + \frac{2}{b} \left[Q_j^i + \left(\frac{\partial Q}{\partial T_F}\right)^i_j T_{F,j}^i + \left(\frac{\partial Q}{\partial T_B}\right)^i_j T_{B,j}^i \right] \right]$	<p>$J = JMAX:$</p> <p>$A(JMAX, 1) = 0$</p> <p>$A(JMAX, 2) = 1$</p> <p>$A(JMAX, 3) = 0$</p> <p>$A(JMAX, 4) = 0$</p> <p>$A(JMAX, 5) = 0$</p> <p>$A(JMAX, 6) = 0$</p> <p>$A(JMAX, 7) = T_{initial}$</p> <p>$B(JMAX, 1) = 0$</p> <p>$B(JMAX, 2) = 0$</p> <p>$B(JMAX, 3) = 0$</p> <p>$B(JMAX, 4) = 0$</p> <p>$B(JMAX, 5) = 1$</p> <p>$B(JMAX, 6) = 0$</p> <p>$B(JMAX, 7) = T_{initial}$</p>

D. STABILITY ANALYSIS

To ensure that the difference scheme chosen to represent the equations will yield stable solutions for fin and fluid temperature distributions, a system stability analysis is performed, as described in Appendix D. For various phase angles (β), unconditional stability requires that the characteristic eigenvalues (λ) of the difference equations are less than or equal to one. The relations for the two eigenvalues derived in Appendix D have been solved as a function of phase angle, assuming a uniform mesh and typical fin and fluid properties (i.e., constant values not dependent on temperature).

The results clearly show that the system of equations is unconditionally stable for all phase angles. As might be expected, when time and spatial increments are decreased, the eigenvalues become even smaller. The resulting eigenvalue for various time and spatial increments are shown as a function of phase angle in Appendix D. The λ versus β curves are symmetric about $\beta = 180$ deg.

IV. RESULTS

Solutions derived from the analytical formulation are obtained and compared with experimental data in this section. Two cases of particular interest are considered. First, comparisons are made with surface temperature data obtained from a clear-air ballistic range shot. Following this, calculations are presented for a typical flight test trajectory in a weather environment.

A. BALLISTIC RANGE TEST CASE

The test data for the ballistic range experiment include actual TCNT surface temperatures located in the stagnation region as a function of time. Prescribed coolant mass flow rates and environmental conditions are then supplied to the numerical solution so that predicted fin temperatures may be compared with measured stagnation temperatures.

The data shown in Fig. 4 indicates that the surface temperatures obtained experimentally are far greater than those determined numerically. Several factors could have caused this discrepancy. The most predominant is the Thom Correlation which represents the source term for subcooled boiling heat transfer. If the correlation causes too much heat to be removed from the fin, predicted fin temperatures will lie below the actual values. Another case was run to establish an upper bound on fin temperatures by using a constant Nusselt number for the source term. The temperature distribution for $Nu = 4.0$ (Fig. 4) lies above the experimental data points. Thus, it appears that because of the influence of the source term, a more realistic correlation for the heat transfer mechanism should yield more accurate results.

The possibility exists that the assumption of a laminar boundary layer also causes deviation from actual surface temperatures. If the non-blown aerodynamic heat flux is greater than that assumed (i.e., a turbulent instead of a laminar heat flux), both fin and fluid temperatures could be higher than

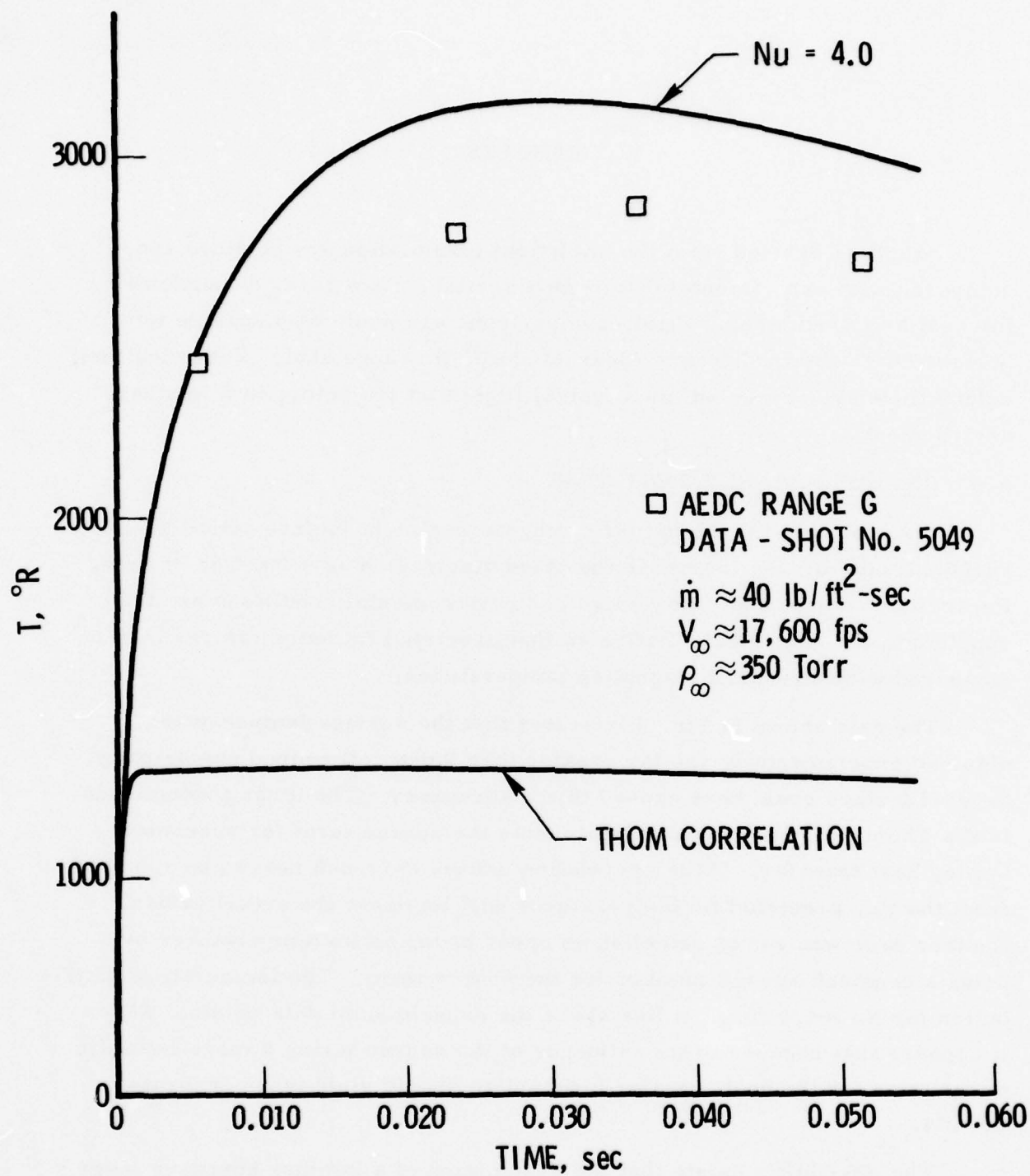


Fig. 4. Fin Surface Temperature for AEDC Ballistic Range

predicted. However, when a turbulent non-blowing flux is incorporated into the solution, the increase in fin temperature is not enough to reproduce the observed temperatures. It may then be concluded that the reported discrepancies are the result of an overly optimistic correlation for the source term.

Even if a realistic correlation for subcooled boiling were incorporated, the numerical solution for fin temperatures would be higher than that indicated by ballistic range data. The difference would arise from the assumption of a gaseous boundary layer. It may be postulated that the liquid particles present in the boundary layer actually reduce driving enthalpy with phase change, lessening the effect of the heat flux at the fin surface so that temperatures are lower. Had this type of result been obtained in the numerical solution, a type of accommodation factor would have to be included to represent the aerodynamic heat flux more accurately.

Since coolant mass flow rates are relatively large for the ballistic range test case, the convective term in the fluid equation may become much larger than the transient term. A case in which the fluid equation is assumed steady state has been run, yielding virtually the same temperature distributions in both fin and fluid as those for the transient case.

B. FLIGHT TRAJECTORY

The computer code was applied to a conventional Kwajalein reentry into a postulated weather environment using a representative stagnation point coolant flow rate. The mass flux of the coolant, shown as a function of altitude in Fig. 5, exerts a stronger influence on the temperatures because of the relatively large range of values it assumes. Fin surface temperatures are seen to rise, then fall off as altitude decreases as shown in Fig. 6, similar to the behavior of coolant flux.

Note that the constant Nusselt number case would predict surface melting in Fig. 6, presumably setting upper and lower bounds for the actual fin temperature distribution. The amount of predicted erosion in

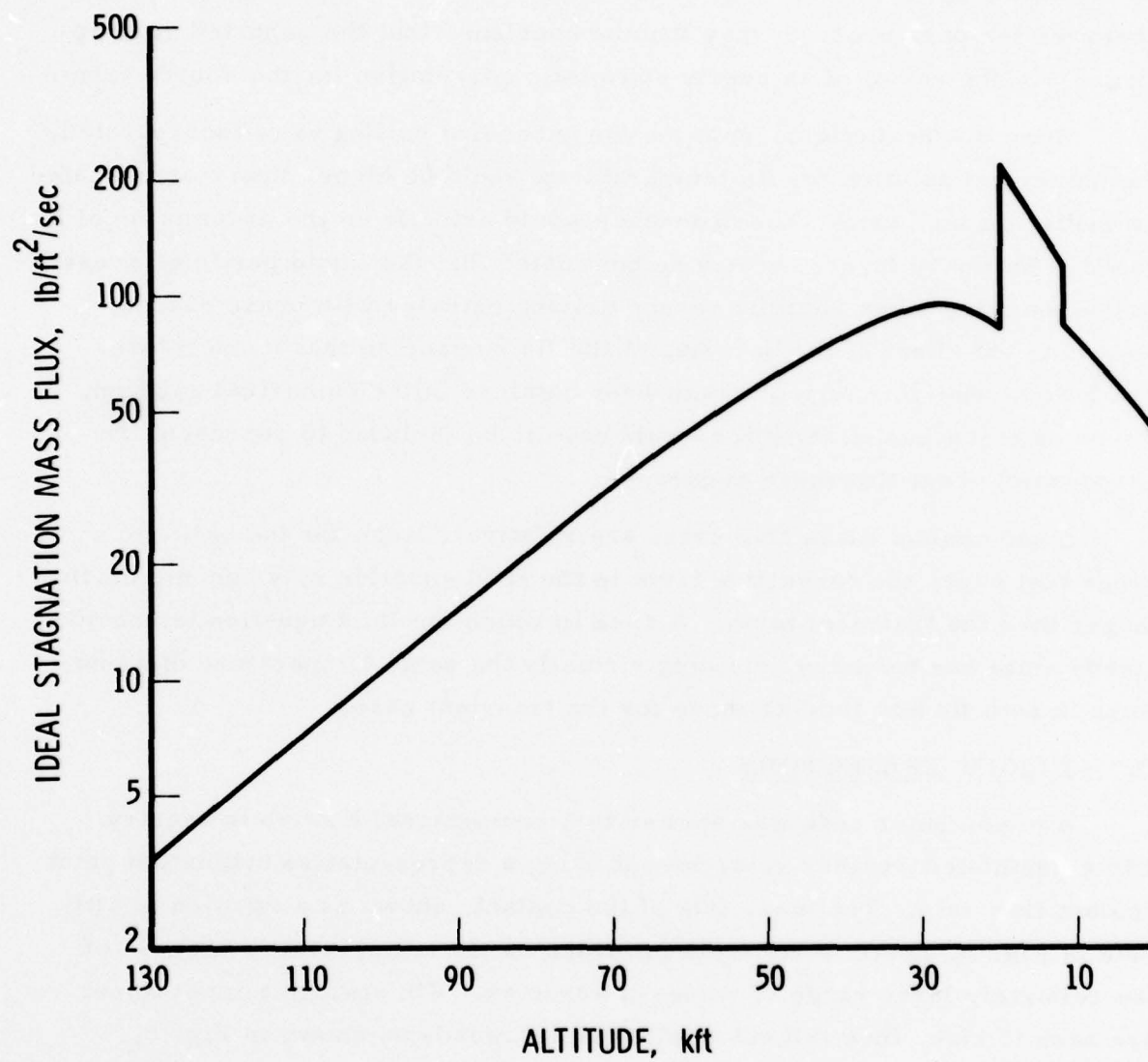


Fig. 5. Stagnation Point Ideal Coolant Requirements
(Kwajalein Mission)

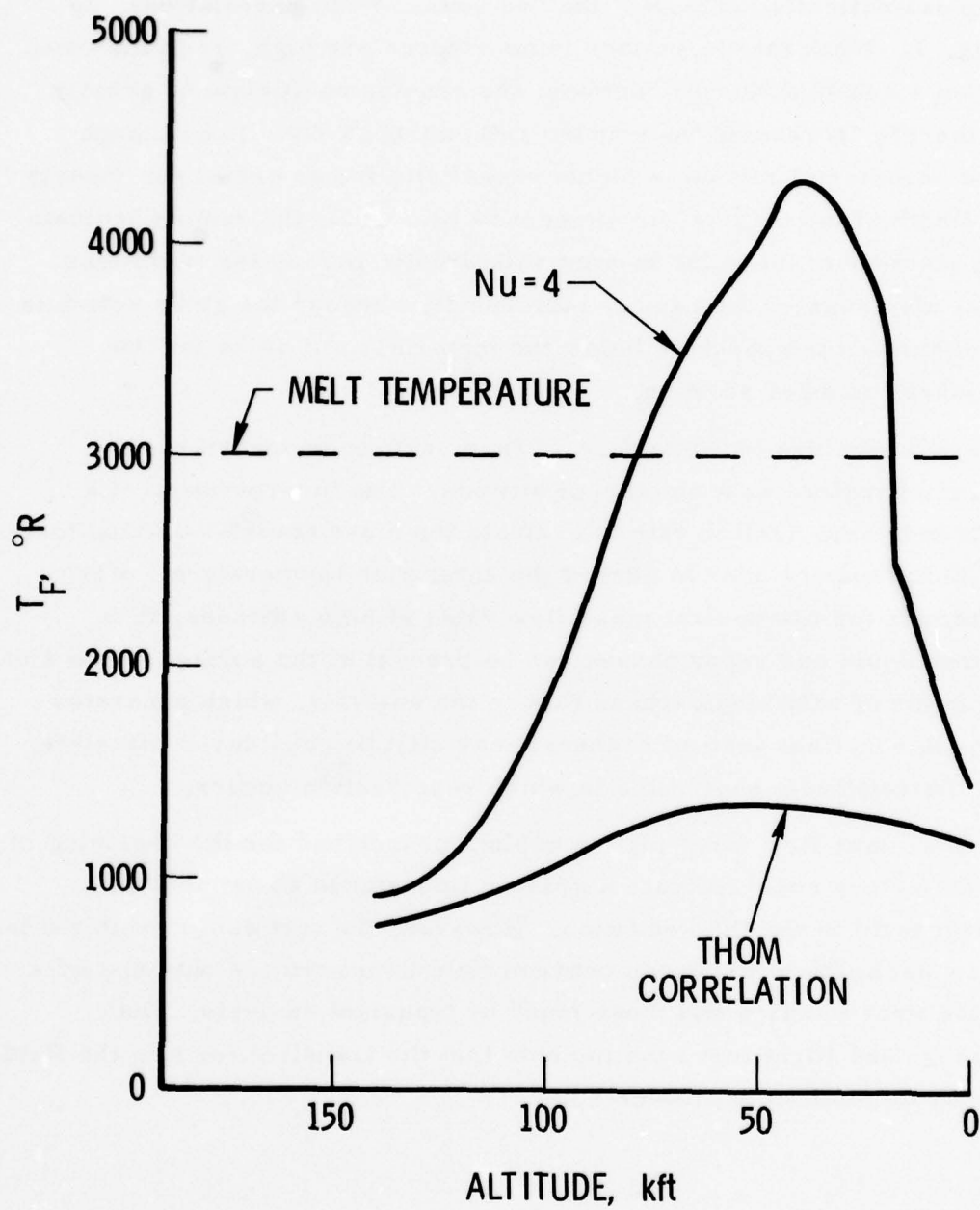


Fig. 6. Fin Surface Temperature for Flight Environment

the nosetip dramatically contrasts the two source term correlations, as seen in Fig. 7. When the fin surface temperatures are high, as in the case arising from a constant Nusselt number, the erosion coefficient is greatly reduced, thereby increasing the erosion rate significantly. Even though the amount of material eroded is highly unrealistic for an actual run (nearly twice the length of the original fin element is removed), the results indicate the strong stability of the solution even with drastic parameter variations. The results also suggest the need to increase flow beyond the given schedule to maintain surface temperature below the material melt value for the constant Nusselt number solution.

Figure 8 provides a comparison of fluid surface temperature and saturation temperature as a function of altitude. The incorporation of a non-equilibrium vaporization rate to evaluate the mass transfer driving force B' allows fluid temperatures to exceed the saturation temperature. While this only occurs for low coolant mass flow rates at high altitudes, it is apparent that liquid and vapor phases can be present at the surface of the slot. The assumption of only single-phase flow in the analysis, which generates two governing equations instead of three, may still be considered plausible, in light of the relatively short time in which vaporization occurs.

The low mass flow rates for the coolant prescribed for the beginning of the flight trajectory could indicate a greater importance associated with the transient term in the fluid equation. However, the test cases exhibited in Fig. 9 show negligible differences between fluid temperatures obtained by a steady-state fluid equation and those found by transient analysis. Both ballistic range and flight test runs indicate that the transient term in the fluid equation may be justifiably eliminated.

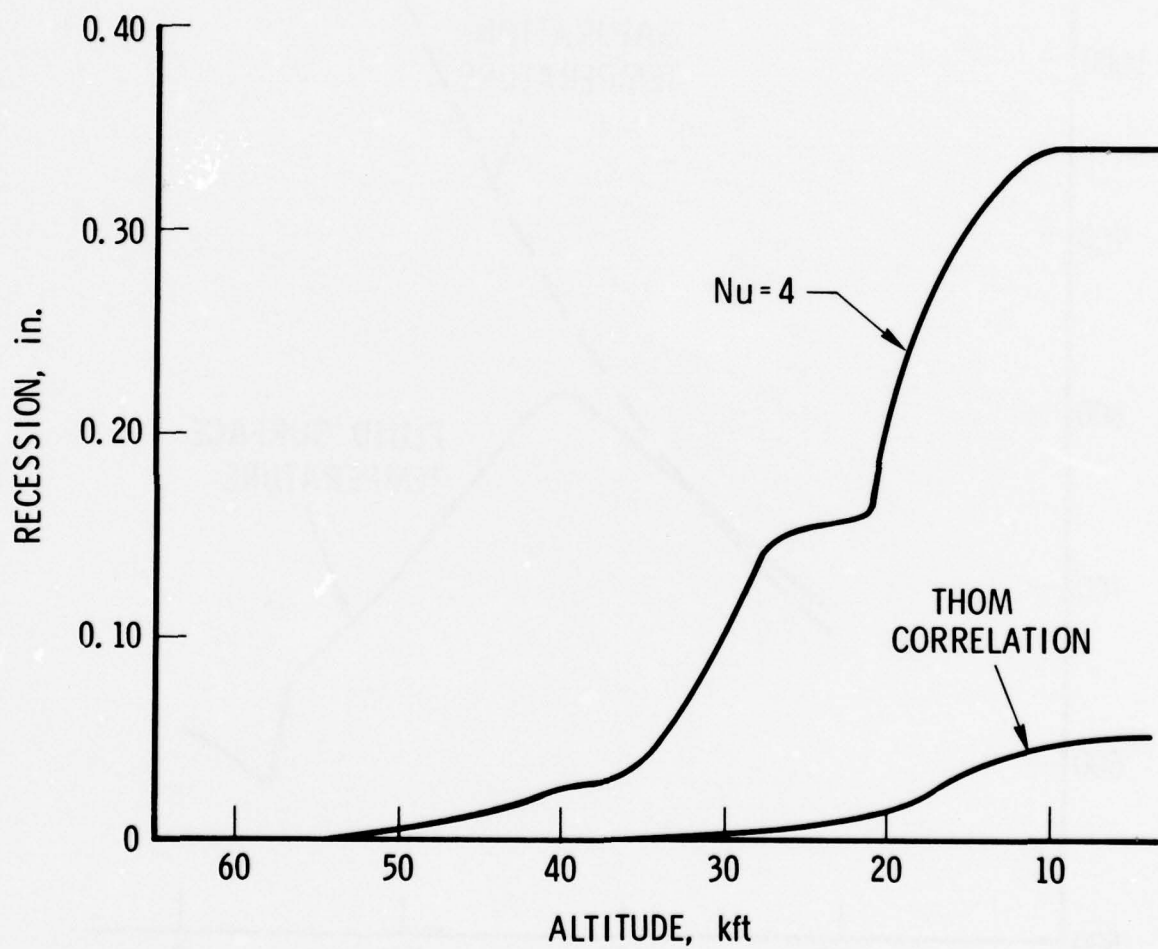


Fig. 7. Influence of Boiling Heat Transfer Model on Fin Erosion for Flight Environment

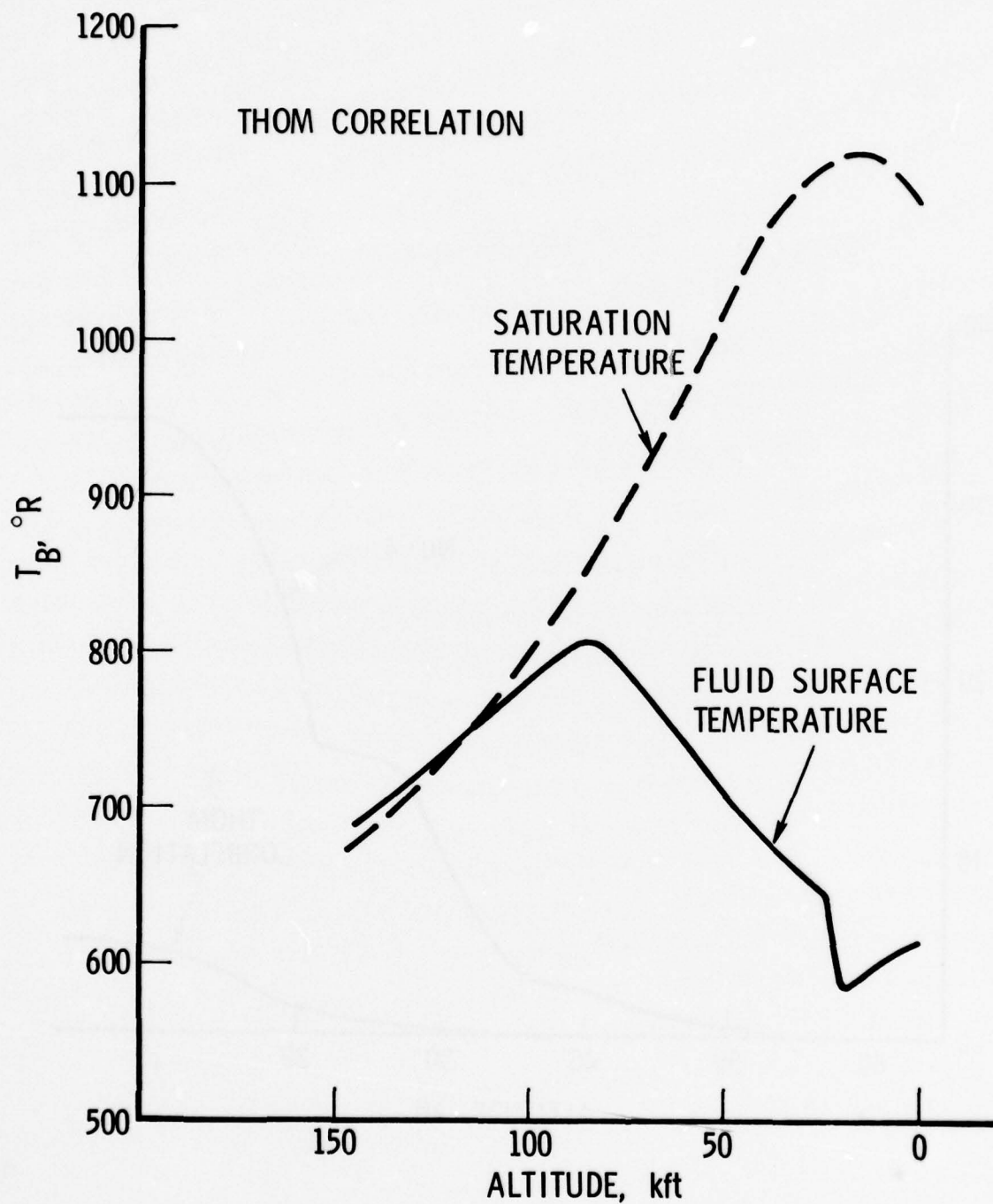


Fig. 8. Comparison of Fluid Surface and Saturation Temperatures for Flight Environment

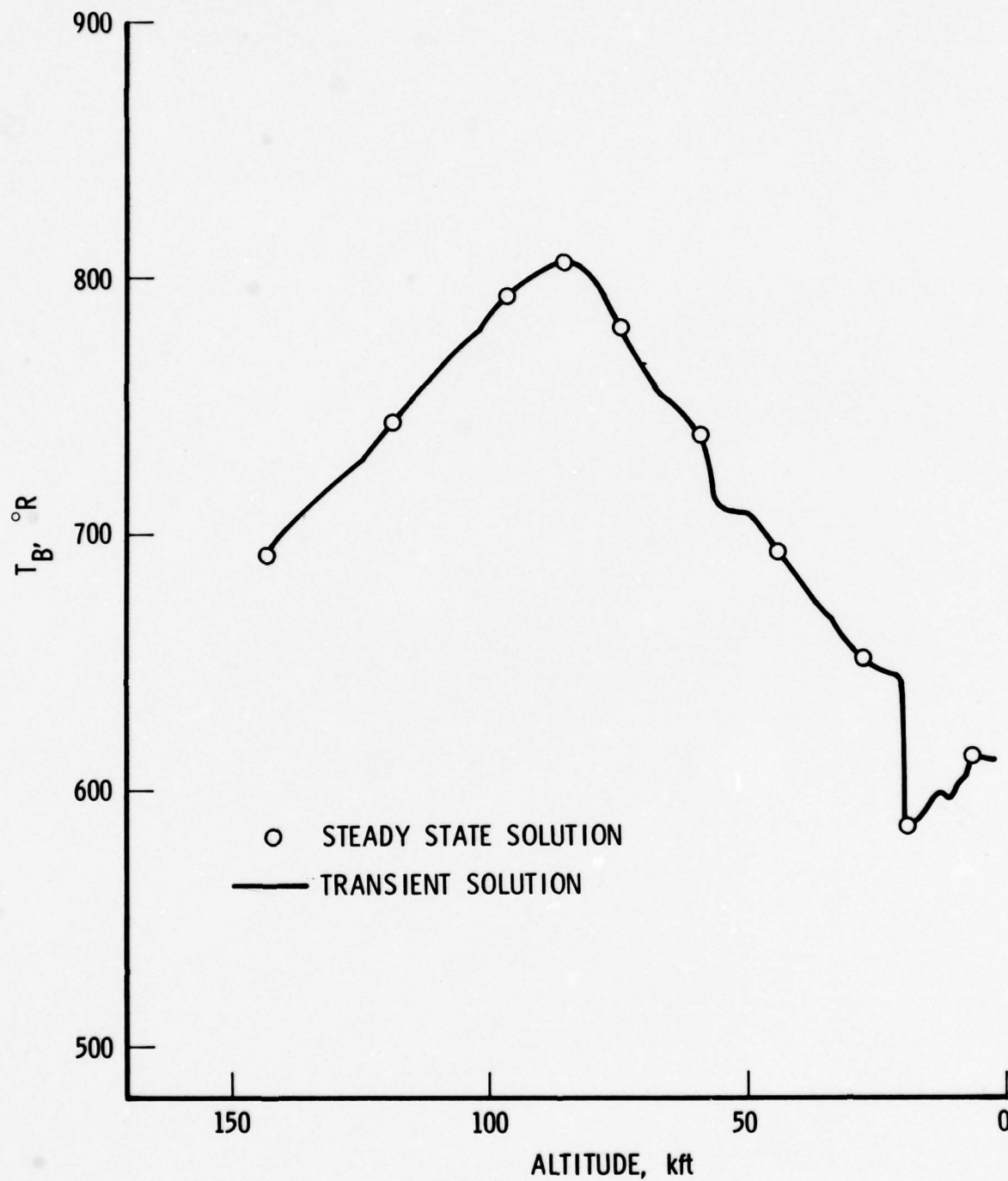


Fig. 9. Comparison of Fluid Surface Temperatures, Transient versus Steady-State Numerical Solution for Flight Environment

V. CONCLUSIONS

The thermodynamic behavior of a discrete injection transpiration-cooled nosetip has been modeled by considering the energy exchange between the metal matrix and coolant for a simple fin and slot combination. The relevant partial differential equations governing the energy transfer in the fin and coolant have been derived and solved numerically using an unconditionally stable implicit finite difference scheme.

While the heat transfer mechanism between fin and fluid accounts for the possibility of subcooled boiling, it is maintained that the bulk of the coolant is in the liquid phase. The analysis treats the governing final equation as such, but in order not to preclude the possibility of two phases, a non-equilibrium vaporization rate of the fluid into the boundary layer is incorporated. It is further assumed that the boundary layer of the nosetip is solely gaseous, so that analysis may be simplified and an upper bound on the surface heat flux may be established.

Comparison of nosetip temperature distributions obtained by numerical means and by experiment indicates that the correlation for subcooled boiling heat transfer is overly optimistic for indepth energy exchange. A more realistic representation might yield surface temperatures closer to the actual values.

While both governing equations are considered to be transient throughout this analysis, a steady-state postulate in the coolant equation yields virtually the same results as the complete transient representation, thereby validating this commonly used assumption.

APPENDIX A. DERIVATION OF GOVERNING EQUATIONS

A. FIN EQUATION

The physical situation depicted in Fig. A-1 represents a fin volume element, located at an arbitrary distance z from the original surface of the nosetip. The coordinate x denotes the distance of the element from the "actual" surface location at some time t , that is, the location of the surface after the fin has begun to erode at a rate \dot{s} .

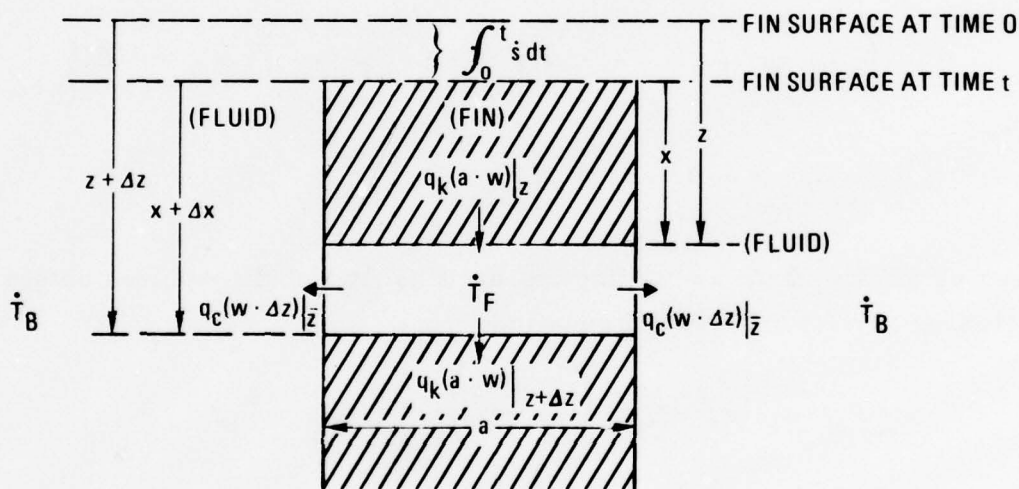


Fig. A-1. Fin Volume Element

The T_F and T_B are used to denote the temperature of the fin and the temperature of the fluid (or "bulk"), respectively. Thus, an energy balance on this volume element will include the following terms

$$q_k = -K_F \frac{\partial T_F}{\partial x}$$

is the rate of heat transfer per unit area due to conduction in the fin (where K_F is the fin thermal conductivity).

$$q_c = h(T_F - T_B)$$

is the rate of heat transfer per unit area due to convection.

The change in sensible energy of the system in time Δt is

$$(\rho_F C_{PF} \cdot a \cdot w \cdot \Delta z) \Big|_{\bar{z}, t} \cdot \left[T_F \Big|_{\bar{z}, t + \Delta t} - T_F \Big|_{\bar{z}, t} \right]$$

so that an overall energy balance yields

$$\begin{aligned} & (\rho_F C_{PF} \cdot a \cdot w \cdot \Delta z) \left[T_F \Big|_{\bar{z}, t + \Delta t} - T_F \Big|_{\bar{z}, t} \right] = \\ & \left(-K_F \frac{\partial T_F}{\partial z} \right) \cdot a \cdot w \cdot \Delta t \Big|_{z, \bar{t}} - \left(-K_F \frac{\partial T_F}{\partial z} \right) \cdot a \cdot w \cdot \Delta t \Big|_{z + \Delta z, \bar{t}} - \\ & 2h \cdot w \cdot \Delta z \cdot \Delta t \left[T_F \Big|_{\bar{z}, \bar{t}} - T_B \Big|_{\bar{z}, \bar{t}} \right] \end{aligned}$$

Dividing by $a \cdot w \cdot \Delta z \Delta t$ and taking the limit as Δt and $\Delta z \rightarrow 0$, we obtain the following partial differential equation

$$\rho_F C_{PF} \frac{\partial T_F}{\partial t} = \frac{\partial}{\partial z} \left(K_F \frac{\partial T_F}{\partial z} \right) + 2 \frac{h}{a} (T_B - T_F) \quad (A-1)$$

In order to incorporate the erosion term in the equation, we perform a transformation to z -coordinates, using the relation

$$z = x + \int_0^t \dot{s} \, dt \quad (\text{or } dz = dx + \dot{s} \, dt) \quad (A-2)$$

Our goal is to transform temperature T_F as a function of z and t to T_F as a function of spatial coordinate x and time \tilde{t} . Thus, if we wish to have

$$T_F(z, t) = T_F(x, \tilde{t})$$

we may then differentiate to obtain

$$\frac{\partial T_F}{\partial z} dz + \frac{\partial T_F}{\partial t} dt = \frac{\partial T_F}{\partial x} dx + \frac{\partial T_F}{\partial \tilde{t}} d\tilde{t}$$

If we let $\tilde{t} \equiv t$ and $d\tilde{t} \equiv dt$, then using Eq. (A-2) we find that

$$\frac{\partial T_F}{\partial z} (dx + \dot{s} dt) + \frac{\partial T_F}{\partial t} dt = \frac{\partial T_F}{\partial x} dx + \frac{\partial T_F}{\partial \tilde{t}} dt$$

or

$$\left[\frac{\partial T_F}{\partial z} \dot{s} + \frac{\partial T_F}{\partial t} \right] dt + \left[\frac{\partial T_F}{\partial z} \right] dx = \left[\frac{\partial T_F}{\partial \tilde{t}} \right] dt + \left[\frac{\partial T_F}{\partial x} \right] dx$$

Equating coefficients, the following relations result

$$\frac{\partial T_F}{\partial z} = \frac{\partial T_F}{\partial x}$$

$$\frac{\partial T_F}{\partial t} = \frac{\partial T_F}{\partial \tilde{t}} - \dot{s} \frac{\partial T_F}{\partial z}$$

Using the transient heat conduction equation for the fin in Eq. (A-1), we obtain

$$\rho_F C_{PF} \frac{\partial T_F}{\partial t} = \frac{\partial}{\partial x} \left(K_F \frac{\partial T_F}{\partial x} \right) + \left(\rho_F C_{PF} \dot{s} \right) \frac{\partial T_F}{\partial x} + 2 \frac{h}{a} (T_B - T_F) \quad (A-3)$$

where t now replaces \tilde{t} . It should be noted that when no erosion takes place, \dot{s} equals zero, and the form of Eq. (A-3) reduces to that of Eq. (A-1).

When erosion of the nosetip surface occurs, examination of the model indicates that the entire fin of length l is shifted downward by the amount $\int_0^t \dot{s} dt$. For the particular application of the transpiration-cooled nosetip, the length l is defined to be the distance from the surface of the fin (before erosion) to the small opening through which coolant is injected, as shown in Fig. A-2.

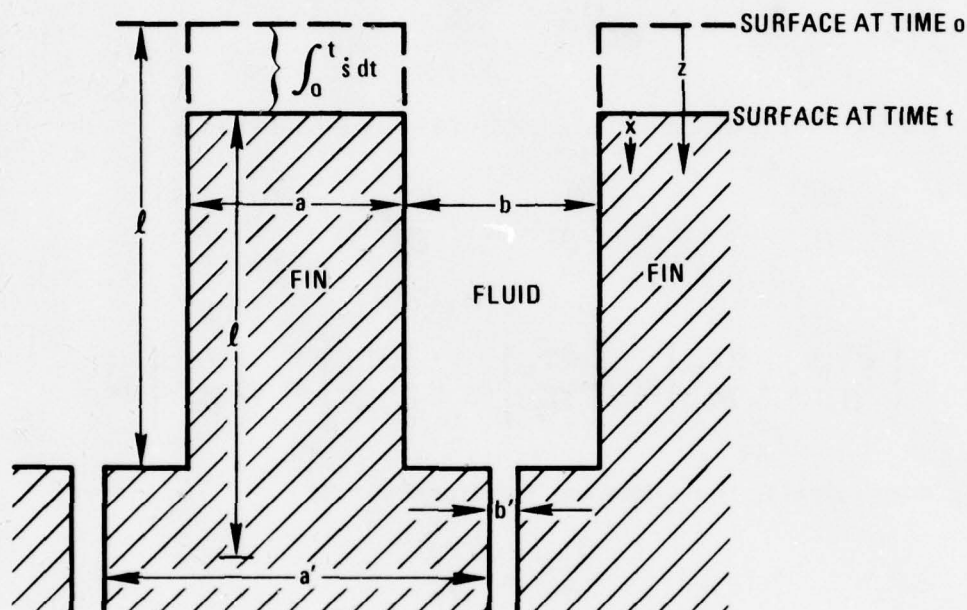
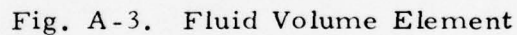


Fig. A-2. Control Volume Geometry

Thus, if the fin is to be considered to have constant length l after erosion takes place, the dimension a in Eq. (A-3) must be replaced by a' for the lower portion of the fin (i. e., for $x = l - \int_0^t \dot{s} dt$ to $x = l$). The same back-face boundary condition would apply as if \dot{s} were zero, since we are assuming the fin to be semi-infinite.

A similar energy balance may be performed on the fluid volume element shown in Fig. A-3, with x- and z-coordinates identical to those of the fin element so that erosion may be taken into account.


$$q_k = -K_B \frac{\partial T_B}{\partial z}$$
$$q_c = h(T_F - T_B)$$
$$\dot{m}C_p T_B$$

- 45 -

An overall energy balance yields the relation

$$\begin{aligned}
 (\rho_B C_{PB} \cdot b \cdot w \cdot \Delta z) \left[T_B \Big|_{\bar{z}, t + \Delta t} - T_B \Big|_{\bar{z}, t} \right] &= \left(-K_B \frac{\partial T_B}{\partial z} \right) \cdot b \cdot w \cdot \Delta t \Big|_{\bar{z}, \bar{t}} - \\
 &- \left(-K_B \frac{\partial T_B}{\partial z} \right) \cdot b \cdot w \cdot \Delta t \Big|_{z + \Delta z, \bar{t}} + \dot{m} C_{PB} \cdot b \cdot w \cdot \Delta t \left(T_B \Big|_{z + \Delta z, \bar{t}} - \right. \\
 &- \left. T_B \Big|_{z, \bar{t}} \right) + 2h \cdot w \cdot \Delta z \left(T_F \Big|_{\bar{z}, \bar{t}} - T_B \Big|_{\bar{z}, \bar{t}} \right) \cdot \Delta t
 \end{aligned}$$

from which the partial differential equation is obtained

$$\rho_B C_{PB} \frac{\partial T_B}{\partial t} = \frac{\partial}{\partial z} \left(K_B \frac{\partial T_B}{\partial z} \right) + (\dot{m} C_{PB}) \frac{\partial T_B}{\partial z} + 2 \cdot \frac{h}{b} (T_F - T_B) \quad (A-4)$$

A coordinate transformation similar to that for the fin equation yields our final result

$$\rho_B C_{PB} \frac{\partial T_B}{\partial t} = \frac{\partial}{\partial x} \left(K_B \frac{\partial T_B}{\partial x} \right) + (\rho_B C_{PB} \dot{s} + \dot{m} C_{PB}) \frac{\partial T_B}{\partial x} + 2 \frac{h}{b} (T_F - T_B) \quad (A-5)$$

Because erosion causes the fin to be "shifted" downward by the amount $\int_0^t \dot{s} dt$, the region of interest in the fluid, also of length l , must translate downward as well. Referring to Fig. A-2, it is apparent that the dimension b in Eq. (A-5) must be replaced by b' for $x = l - \int_0^t \dot{s} dt$ to $x = l$. It is clear that, since \dot{m} is defined as the mass flow rate of the coolant per unit area, a different value \dot{m}' should be substituted into the equation for $l - \int_0^t \dot{s} dt < x \leq l$. From continuity, this new mass flow is found to be $\dot{m}' = \dot{m}(b/b')$.

In the derivation of Eq. (A-5), the fluid was assumed to be incompressible such that work due to volumetric changes is negligible. The fluid velocity is assumed constant such that viscous dissipation can be ignored.

APPENDIX B. VAPORIZATION FROM A LIQUID WATER SURFACE

The mass transfer parameter B' is required to determine the reduction in aerodynamic heat flux due to coolant vaporization at the slot surface. The mass transfer parameter is obtained from the analysis given in this appendix.

The problem is to determine the vaporization from a liquid water surface over which an air boundary layer is flowing. In order to simplify the analysis, the usual assumptions of unity Prandtl and Lewis number and equal diffusion coefficients are invoked. With these assumptions, the elemental mass fractions at the surface are obtained from the wall boundary conditions for the elemental conservation equations in terms of the mass transfer parameter.

$$\tilde{K}_{O_w} = \frac{\tilde{K}_{O_e} + \frac{16}{18} B'}{1 + B'} \quad \tilde{K}_{O_e} = 0.232$$

$$\tilde{K}_{N_w} = \frac{\tilde{K}_{N_e}}{1 + B'} \quad \tilde{K}_{N_e} = 0.768$$

$$\tilde{K}_{H_w} = \frac{\frac{2}{18} B'}{1 + B'}$$

$$B' \equiv \frac{\dot{m}}{\rho_e u_e C_H} \quad (B-1)$$

where subscripts w and e refer to wall and boundary layer edge conditions, respectively, and superscript tilde refers to element mass fractions.

Assuming that the surface temperature is low enough to preclude dissociation reactions, the gas phase at the wall consists solely of molecular oxygen, nitrogen, and steam. Elemental conservation at the wall yields

$$\begin{aligned}\tilde{K}_{N_w} &= K_{N_2} \\ \tilde{K}_{O_w} &= K_{O_2} + \frac{16}{18} K_{H_2O} \\ \tilde{K}_{H_w} &= \frac{2}{18} K_{H_2O}\end{aligned}\tag{B-2}$$

The sum of the partial pressures must equal the mixture pressure

$$P_{N_2} + P_{O_2} + P_{H_2O} = P\tag{B-3}$$

The partial pressures are related to the species mass fractions as follows:

$$\begin{aligned}P_{N_2} &= \frac{PMK_{N_2}}{28} & P_{O_2} &= \frac{PMK_{O_2}}{32} \\ P_{H_2O} &= \frac{PMK_{H_2O}}{18}\end{aligned}\tag{B-4}$$

If it is assumed that the vaporization reaction is in equilibrium such that the water vapor partial pressure is identical to its equilibrium vapor pressure (i.e., $P_{H_2O} = P_{H_2O}^v$), the mass transfer parameter may be obtained from the foregoing expression as

$$B'_{eq} = \frac{18\beta P_{H_2O}^v}{P - P_{H_2O}^v} \quad \beta \equiv \frac{\tilde{K}_{N_e}}{28} + \frac{\tilde{K}_{O_e}}{32}\tag{B-5}$$

where β was defined for notational convenience.

Since the vapor pressure is a known function of temperature, the equilibrium value of B' is easily computed for specified values of surface temperature and pressure. The equilibrium mass transfer parameter is undefined for surface temperatures greater than the saturation temperature (i.e., $P_{H_2O}^v > P$). Thus, the use of the equilibrium assumption would constrain the solution for the surface coolant temperature to always be less than the saturation value. In some instances this is physically unrealistic, and the mass transfer parameter will be obtained from a non-equilibrium assumption.

The non-equilibrium vaporization rate is modeled using the Knudsen-Langmuir equation, which is given as

$$\dot{m} = \alpha \sqrt{\frac{M}{RT}} \left(P_{H_2O}^v - P_{H_2O} \right) \quad (B-6)$$

where α is the vaporization coefficient, and M is the molecular weight of water vapor.

Using the definition of B' and dividing through by the heat flux yields

$$B' = \frac{G \left(P_{H_2O}^v - P_{H_2O} \right)}{\frac{C_H}{C_{H_0}}} \quad (B-7)$$

$$G \equiv \frac{\alpha}{\rho_e u_e C_{H_0}} \sqrt{\frac{M}{RT}}$$

This equation, along with the previously obtained expressions, yields a nonlinear algebraic equation for B' .

$$B' \left(\beta + \frac{B'}{18} \right) \frac{C_H}{C_{H_0}} + \frac{GB'}{18} \left(P - P_{H_2O}^v \right) = G\beta P_{H_2O}^v \quad (B-8)$$

Since the ratio of blowing to non-blowing Stanton number is presumed to be a known function of B' , this equation may be solved iteratively for B' for specified values of surface temperature, pressure, and non-blowing heat flux (i.e., $\rho_e u_e C_{H_o}$). The Stanton number expression used in this report is given as

$$\frac{C_H}{C_{H_o}} = \frac{\ln(1 + \lambda B')}{\lambda B'} ; \quad \lambda = 1.28$$

As equilibrium is approached (i.e., $C_{H_o} \rightarrow 0$), Eq. (B-8) yields exactly the value of Eq. (B-5) for B' . Furthermore, Eq. (B-8) is well defined at the saturation temperature, thereby allowing solutions for surface coolant temperature in excess of the saturation value.

The required value of vaporization coefficient was obtained⁵ and is given as $\alpha = 0.04$.

Some typical values for B' are shown in Fig. B-1 for a pressure of 100 atm for both the equilibrium and non-equilibrium case.

⁵ John P. Hirth, "Evaporation and Sublimation Mechanisms," The Characterization of High Temperature Vapors, Chapter 15, ed. T. L. Margrave, John Wiley and Sons, Inc., New York (1967).

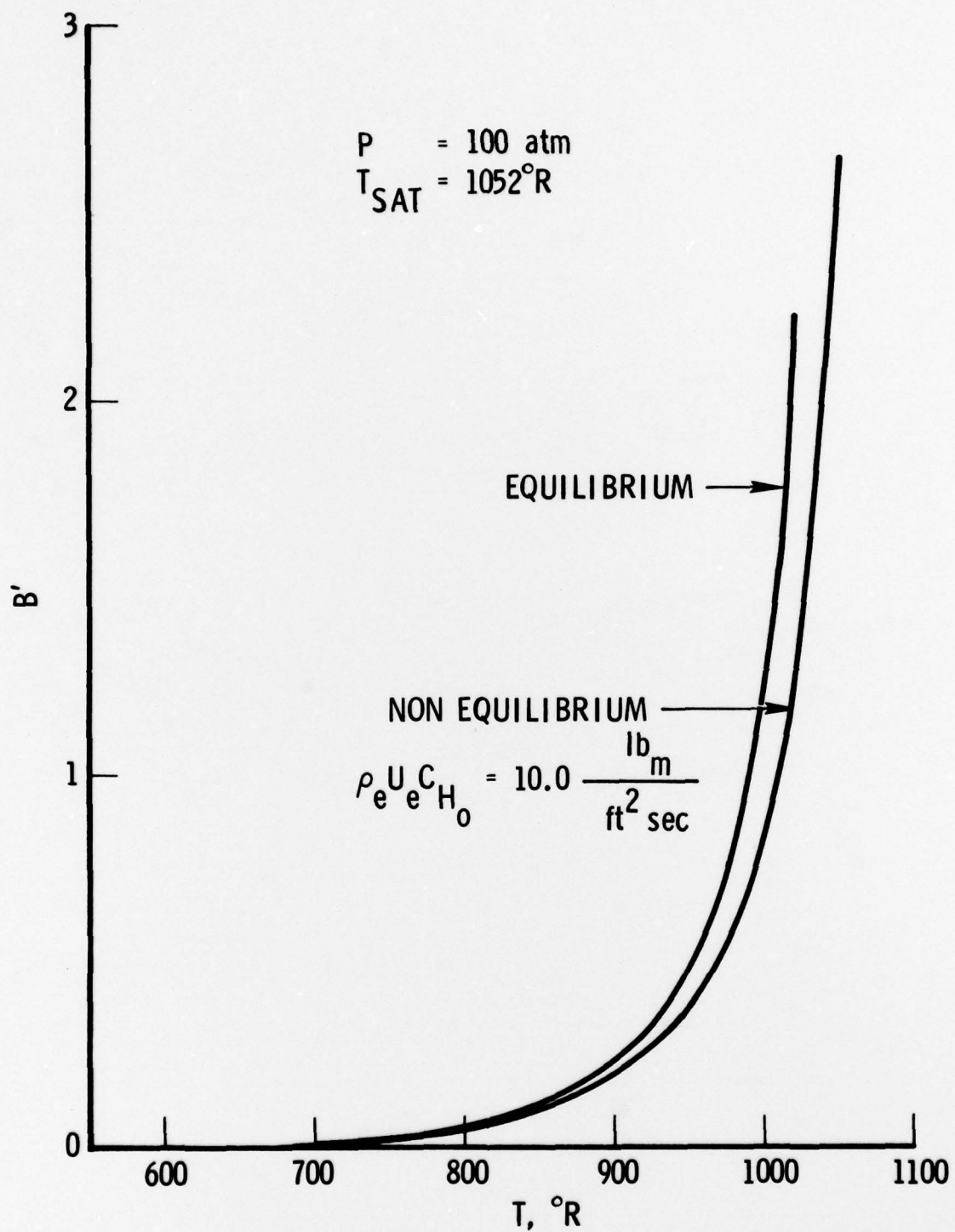


Fig. B-1. Mass Transfer Parameter for Water Vaporization

APPENDIX C. QUASILINEARIZED FORMULATION OF PARAMETERS

The two parameters in the governing partial differential equations which are strong functions of temperature are Q , the coupling heat transfer source term in both equations, and \dot{q}_{net} , the fin surface heat flux which enters into one boundary condition. When the governing equations are represented in finite difference form, it is necessary that these two terms in particular are evaluated at "future" time levels to ensure consistency. Hence, a technique is incorporated to evaluate the terms iteratively. The terms Q and \dot{q}_{net} will be represented at future time levels by the method of quasilinearization, which consists of simply expanding the terms in a Taylor series.

A. THE SOURCE TERM Q

The source term evaluated at iteration level $i+1$ is

$$Q_j^{i+1} = Q_j^i + \left(\frac{\partial Q}{\partial T_F} \right)_j^i (T_{F_j}^{i+1} - T_{F_j}^i) + \left(\frac{\partial Q}{\partial T_B} \right)_j^i (T_{B_j}^{i+1} - T_{B_j}^i) \quad (\text{C-1})$$

Since Q is represented by two different relations, dependent upon the regime of the fin temperature, the derivatives take two different forms:

If $T_{F_j}^i \leq T_{\text{sat}}$ (fluid)

$$Q_j^i = h (T_{B_j}^i - T_{F_j}^i) \quad \text{where } h = 4 \cdot K_B / D_H$$

$$\left(\frac{\partial Q}{\partial T_F} \right)_j^i = \frac{-4 \cdot K_B}{D_H}$$

and

$$\left(\frac{\partial Q}{\partial T_B} \right)_j^i = \frac{4 \cdot K_B}{D_H} \quad (\text{C-2})$$

$$\text{If } T_{F_j}^i > T_{\text{sat}} \text{ (fluid)}$$

$$Q_j^i = 0.0536 e^{(P/630)} \left(T_{F_j}^i - T_{\text{sat}} \right)^2 \quad \text{where } P \text{ is in psia;}$$

$$\left(\frac{\partial Q}{\partial T_F} \right)_j^i = 2(0.0536) e^{(P/630)} \left(T_{F_j}^i - T_{\text{sat}} \right);$$

and

$$\left(\frac{\partial Q}{\partial T_B} \right)_j^i = 0 \quad (\text{C-3})$$

When the fin temperature exceeds the fluid saturation temperature, the relation which yields the maximum value of Q is chosen to represent the source term. In this case, the associated derivatives for the particular Q relation are substituted into Eq. (C-1).

B. THE SURFACE HEAT FLUX \dot{q}_{net}

The net heat flux impinging on the surface of the fin may be divided into three major components. These are (a) the fluxes due to aerodynamic heating, (b) particle heating, and (c) radiation. The representation of the surface boundary condition is

$$-K_F \frac{\partial T_F}{\partial x} = \dot{q}_{\text{net}}^i + \left(\frac{\partial \dot{q}_{\text{net}}}{\partial T_F} \right)_1^i \left(T_{F_1}^{i+1} - T_{F_1}^i \right) + \left(\frac{\partial \dot{q}_{\text{net}}}{\partial T_B} \right)_1^i \left(T_{B_1}^{i+1} - T_{B_1}^i \right) \quad (\text{C-4})$$

where

$$\dot{q}_{\text{net}}^i = \dot{q}_{\text{aero}}^i + \dot{q}_{\text{part}}^i - \dot{q}_{\text{rad}}^i$$

$$\dot{q}_{\text{aero}}^i = \dot{q}_o \left(1 - \frac{h_w}{H_R} \right) \frac{C_H}{C_{H_o}}$$

$$\dot{q}_{\text{part}}^i = \frac{1}{2} \alpha \rho_{\text{LWC}} (U_\infty)^3$$

$$\dot{q}_{\text{rad}}^i = \epsilon \sigma (T_{F1}^i)^4$$

The particle heat flux is independent of either temperature, but both \dot{q}_{aero} and \dot{q}_{rad} enter into the evaluation of the derivatives

$$\left(\frac{\partial \dot{q}_{\text{net}}}{\partial T_F} \right)_1^i = \left(\frac{\partial \dot{q}_{\text{aero}}}{\partial T_F} \right)_1^i - \left(\frac{\partial \dot{q}_{\text{rad}}}{\partial T_B} \right)_1^i$$

$$\left(\frac{\partial \dot{q}_{\text{net}}}{\partial T_B} \right)_1^i = \left(\frac{\partial \dot{q}_{\text{aero}}}{\partial T_B} \right)_1^i$$

To obtain the derivatives of aerodynamic heat flux, it must first be determined how the term is dependent on temperature. For the relation

$$\dot{q}_{\text{aero}} = \dot{q}_o \left(1 - \frac{h_w}{H_R} \right) \frac{C_H}{C_{H_o}}$$

the terms \dot{q}_o and H_R are functions of the local boundary layer conditions and therefore independent of T_F or T_B , the term h_w is found by

$$h_w = RT_F \left[\frac{K_{O_2}}{32} \left(\frac{H}{RT_F} \right)_{O_2} + \frac{K_{N_2}}{28} \left(\frac{H}{RT_F} \right)_{N_2} + \frac{K_{H_2O}}{18} \left(\frac{H}{RT_F} \right)_{H_2O} \right]$$

with

$$K_{O_2} = \frac{\tilde{K}_{O_e}}{1 + B'}, \quad K_{N_2} = \frac{\tilde{K}_{N_e}}{1 + B'}, \quad \text{and } K_{H_2O} = \frac{B'}{1 + B'}$$

and

$$\frac{C_H}{C_{H_o}} = \frac{\ln(\lambda B' + 1)}{\lambda B'} \quad (\lambda = 1.28)$$

It is apparent that h_w is a function of the fin temperature T_F . Since the mass transfer driving force B' is solved iteratively using the relation

$$\left(\beta + \frac{B'}{18} \right) \frac{\ln(\lambda B' + 1)}{\lambda} + G \frac{B'}{18} (P - P_{H_2O}^v) = G \beta P_{H_2O}^v$$

where

$$G \equiv \frac{128.0536 \alpha}{\rho_e u_e C_{H_o}} \sqrt{\frac{M}{RT_B}}$$

$$\beta \equiv \frac{\tilde{K}_{N_e}}{28} + \frac{\tilde{K}_{O_e}}{32}$$

It can be seen that both h_w and C_H/C_{H_o} are functions of the fluid temperature T_B . Thus, the aerodynamic heat flux derivatives become

$$\frac{\partial \dot{q}_{aero}}{\partial T_B} = \dot{q}_o \frac{\partial \left(\frac{C_H}{C_{H_o}} \right)}{\partial T_B} - \frac{\dot{q}_o}{H_R} \left[h_w \frac{\partial \left(\frac{C_H}{C_{H_o}} \right)}{\partial T_B} + \left(\frac{C_H}{C_{H_o}} \right) \frac{\partial h_w}{\partial T_B} \right] \quad (C-4)$$

and

$$\frac{\partial \dot{q}_{aero}}{\partial T_F} = \frac{-\dot{q}_o}{H_R} \left(\frac{C_H}{C_{H_o}} \right) \frac{\partial h_w}{\partial T_F} \quad (C-5)$$

All of the derivatives in Eqs. (C-4) and (C-5) may be evaluated in closed form.

APPENDIX D. STABILITY ANALYSIS FOR SYSTEM OF EQUATIONS

A. GENERAL

A stability analysis for the coupled systems of difference equations obtained in Section III will provide information about the constraints (if any) imposed on selection of time and spatial increments. For a system of equations to be unconditionally stable, it is required that the characteristic eigenvalues (λ) be less than or equal to unity for all values of the coefficients. The analysis herein has assumed the coefficients in the governing equations to be extreme "worst case" values, and the spatial increments to be uniform ($R = 1$).

The fluid and fin difference equations may be represented as follows for stability considerations.

1. FLUID EQUATION

$$T_{B_j}^{n+1} - T_{B_j}^n = A \left[T_{B_{j+1}}^{n+1} - T_{B_j}^{n+1} \right] + B \left[T_{F_j}^{n+1} - T_{B_j}^{n+1} \right]$$

where

$$A \equiv \frac{(\dot{m}C_{PB} + \rho_B C_{PB} \dot{s}) \Delta t}{\rho_B C_{PB} \Delta x}, \quad A > 0$$

$$B \equiv \frac{2h\Delta t}{\rho_B C_{PB} b}, \quad B > 0 \quad (D-1)$$

2. FIN EQUATION

$$T_{F_j}^{n+1} - T_{F_j}^n = C \left[T_{F_{j+1}}^{n+1} - 2T_{F_j}^{n+1} + T_{F_{j-1}}^{n+1} \right] + D \left[T_{F_{j+1}}^{n+1} - T_{F_{j-1}}^{n+1} \right] + E \left[T_{B_j}^{n+1} - T_{F_j}^{n+1} \right] \quad (D-2)$$

where

$$C \equiv \frac{K_F \Delta t}{\rho_F C_{PF} (\Delta x)^2}, \quad C > 0$$

$$D \equiv \frac{\left(\dot{\rho}_F C_{PF} + \frac{\partial K_F}{\partial x} \right) \Delta t}{2 \Delta x \rho_F C_{PF}}, \quad D > 0$$

$$E \equiv \frac{2h \Delta t}{\rho_F C_{PF} a}, \quad E > 0$$

Since constant coefficients in the difference equations are assumed, the need for iterations is eliminated, and the unknown temperatures are to be found at time level $n+1$.

In accordance with Richtmyer and Morton⁴, it may be assumed that the set of solutions to these simultaneous equations takes the form

$$T_{B_j}^n = G_1^n \epsilon^j \quad \text{and} \quad T_{F_j}^n = G_2^n \epsilon^j$$

where G_1^n and G_2^n are some functions of x and t raised to the n^{th} power and $\epsilon = \cos \beta + i \sin \beta$, a function of the system phase angle β (ϵ is raised to the power j).

Plugging these solutions for temperature into Eqs. (D-1) and (D-2), and using the identities

$$\epsilon - \frac{1}{\epsilon} = 2i \sin \beta$$

and

$$\epsilon + \frac{1}{\epsilon} = 2 \cos \beta$$

the following is derived for the fluid and fin equations

$$G_2^{n+1} = \frac{G_1^{n+1} [1 + B - A(\cos \beta + i \sin \beta - 1)] - G_1^n}{B} \quad (D-3)$$

$$G_1^{n+1} = \frac{G_2^{n+1} [1 + E - 2C(\cos \beta - 1) - i(2D \sin \beta)] - G_2^n}{E} \quad (D-4)$$

These equations may be solved simultaneously to obtain relations for the functions G_1 and G_2 at time level $n+1$ in terms of the functions at time level n

$$\begin{bmatrix} G_1^{n+1} \\ G_2^{n+1} \end{bmatrix} = \begin{bmatrix} a_{11} & a_{12} \\ a_{21} & a_{22} \end{bmatrix} \begin{bmatrix} G_1^n \\ G_2^n \end{bmatrix}$$

where

$$a_{11} = \frac{[1 - E - 2C(\cos \beta - 1) - i(2D \sin \beta)]}{R - iI}$$

$$a_{12} = \frac{B}{R - iI}$$

$$a_{21} = \frac{E}{R - iI}$$

$$a_{22} = \frac{[1 + B - A(\cos \beta - 1) - i(A \sin \beta)]}{R - iI}$$

with

$$R \equiv [1 + B - A(\cos\beta - 1)] [1 + E - 2C(\cos\beta - 1)] - (A \sin\beta)(2D \sin\beta) - BE$$

$$I \equiv (A \sin\beta)[1 + E - 2C(\cos\beta - 1)] + [1 + B - A(\cos\beta - 1)] (2D \sin\beta)$$

The matrix containing the a_{kl} coefficients is known as the amplification matrix. It is the eigenvalues (λ) of this matrix which yield the important information concerning system stabilization

$$\begin{vmatrix} a_{11} - \lambda & a_{12} \\ a_{21} & a_{22} - \lambda \end{vmatrix} = 0$$

The final polynomial to be solved for the eigenvalues is

$$\lambda^2 - \lambda \left[\frac{x_1 + i x_2}{R^2 + I^2} \right] + \left[\frac{R + iI}{R^2 + I^2} \right] = 0 \quad (D-5)$$

where

$$x_1 = R \left\{ 2 + B + E - (2C + A)(\cos\beta - 1) \right\} - I(2D + A)\sin\beta$$

and

$$x_2 = -R(2D + A)\sin\beta + I \left\{ 2 + B + E - (2C + A)(\cos\beta - 1) \right\}$$

If $|\lambda| \leq 1$ for all values of A, B, C, D, and E, and for $0^\circ \leq \beta < 360^\circ$, then it may be concluded that the system is unconditionally stable. Since extreme constant parameters in this system of equations has been assumed, the terms A - E may be varied by changing the time and/or spatial increments.

For the case where $\beta = 0^\circ$, Eq. (D-5) reduces considerably, and yields the two eigenvalues

$$\lambda_{1,2} = \frac{1}{1 + B + E}, \quad 1$$

Since the coefficients B and E are always greater than zero, the stability criterion is unconditionally satisfied at $\beta = 0^\circ$.

When $\beta \neq 0^\circ$, the solutions for λ are found by complex analysis. The resulting eigenvalues are then

$$\lambda_1 = \frac{1}{2} \sqrt{\frac{(x_1^2 + x_2^2)}{(R^2 + I^2)^2} + r - \frac{2\sqrt{r}}{R^2 + I^2} \left(x_1 \cos \frac{\theta}{2} + x_2 \sin \frac{\theta}{2} \right)} \quad (D-6)$$

$$\lambda_2 = \frac{1}{2} \sqrt{\frac{(x_1^2 + x_2^2)}{(R^2 + I^2)^2} + r + \frac{2\sqrt{r}}{R^2 + I^2} \left(x_1 \cos \frac{\theta}{2} + x_2 \sin \frac{\theta}{2} \right)} \quad (D-7)$$

where

$$r \equiv \sqrt{a^2 + b^2}$$

$$\theta \equiv \tan^{-1} \frac{b}{a}$$

with

$$a = \frac{x_1^2 - x_2^2}{(R^2 + I^2)^2} - \frac{4R}{R^2 + I^2};$$

$$b = \frac{2x_1 x_2}{(R^2 + I^2)^2} - \frac{4I}{R^2 + I^2};$$

and x_1 , x_2 , R , and I are the same as previously given.

When combinations of Δt and Δx are substituted into these relations for β varying between 0 deg and 360 deg, a complete picture of the system stability is obtained. In every instance, the computer solution shows that each eigenvalue is less than unity, except at $\beta = 0^\circ$, when λ_2 becomes equal to one. The case when both eigenvalues approach unity closest is for a very small time increment and a very large spatial increment ($\Delta t = 0.00001$ sec, $\Delta x = 0.1$ ft). Yet the eigenvalues always remain less than or equal to unity, indicating that the governing difference equations are unconditionally stable. A sample plot of λ versus β is shown in Fig. D-1.

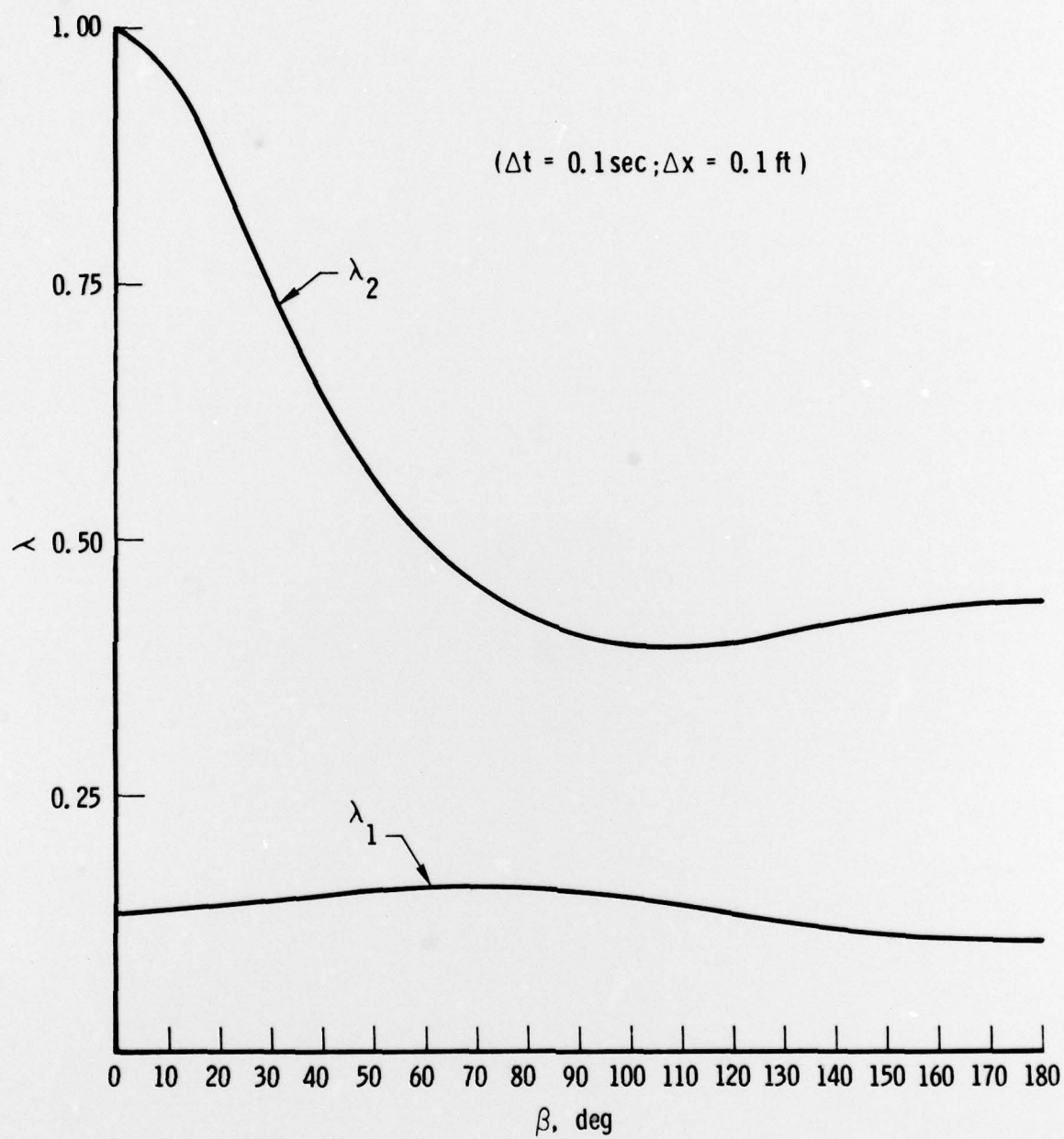


Fig. D-1. Eigenvalues versus Phase Angle β

NOMENCLATURE

a	fin width
B'	mass transfer parameter [defined in Eq. (6)]
b	slot width
C_P	specific heat
H_R	recovery enthalpy
$(H/RT)_i$	normalized enthalpy of species i
K	thermal conductivity
K_i	mass fraction of species i
\dot{m}	coolant mass flow rate per unit area
R	universal gas constant
\dot{s}	fin surface recession rate
T	temperature
t	time
l	slot depth
ρ	density
$\rho_{e^u}^u C_H$	cold wall, blowing heat flux parameter = \dot{q}/H_R
$\rho_{e^u}^u C_{H_O}$	cold wall, nonblowing heat flux parameter = \dot{q}_o/H_R

Subscripts

B	coolant properties
F	fin properties
W	wall values